Update of AAPM Task Group No. 43 Report: A revised AAPM protocol for brachytherapy dose calculations

Mark J. Rivard
Department of Radiation Oncology, Tufts-New England Medical Center, Boston, Massachusetts 02111

Bert M. Coursey
Ionizing Radiation Division, National Institute of Standards and Technology, Gaithersburg, Maryland 20899

Larry A. DeWerd
Accredited Dosimetry and Calibration Laboratory, University of Wisconsin, Madison, Wisconsin 53706

William F. Hanson
Radiological Physics Center, M. D. Anderson Cancer Center, Houston, Texas 77030

M. Saiful Huq
Kimmel Cancer Center of Jefferson Medical College, Thomas Jefferson University, Philadelphia, Pennsylvania 19107

Geoffrey S. Ibbott
Radiological Physics Center, M. D. Anderson Cancer Center, Houston, Texas 77030

Michael G. Mitch
Ionizing Radiation Division, National Institute of Standards and Technology, Gaithersburg, Maryland 20899

Ravinder Nath
Department of Therapeutic Radiology, Yale University, New Haven, Connecticut 06510

Jeffrey F. Williamson
Chair, Low-energy Interstitial Brachytherapy Dosimetry subcommittee of the Radiation Therapy Committee, Department of Radiation Oncology, Virginia Commonwealth University, Richmond, Virginia 23298

(Received 22 August 2003; revised 11 December 2003; accepted for publication 16 December 2003; published 27 February 2004)

Since publication of the American Association of Physicists in Medicine (AAPM) Task Group No. 43 Report in 1995 (TG-43), both the utilization of permanent source implantation and the number of low-energy interstitial brachytherapy source models commercially available have dramatically increased. In addition, the National Institute of Standards and Technology has introduced a new primary standard of air-kerma strength, and the brachytherapy dosimetry literature has grown substantially, documenting both improved dosimetry methodologies and dosimetric characterization of particular source models. In response to these advances, the AAPM Low-energy Interstitial Brachytherapy Dosimetry subcommittee (LIBD) herein presents an update of the TG-43 protocol for calculation of dose-rate distributions around photon-emitting brachytherapy sources. The updated protocol (TG-43U1) includes (a) a revised definition of air-kerma strength; (b) elimination of *apparent activity* for specification of source strength; (c) elimination of the anisotropy constant in favor of the distance-dependent one-dimensional anisotropy function; (d) guidance on extrapolating tabulated TG-43 parameters to longer and shorter distances; and (e) correction for minor inconsistencies and omissions in the original protocol and its implementation. Among the corrections are consistent guidelines for use of point- and line-source geometry functions. In addition, this report recommends a unified approach to comparing reference dose distributions derived from different investigators to develop a single critically evaluated consensus dataset as well as guidelines for performing and describing future theoretical and experimental single-source dosimetry studies. Finally, the report includes consensus datasets, in the form of dose-rate constants, radial dose functions, and one-dimensional (1D) and two-dimensional (2D) anisotropy functions, for all low-energy brachytherapy source models that met the AAPM dosimetric prerequisites [Med. Phys. **25**, 2269 (1998)] as of July 15, 2001. These include the following ^{125}I sources: Amersham Health models 6702 and 6711, Best Medical model 2301, North American Scientific Inc. (NASI) model MED3631-A/M, Bebig/Theragenics model I25.S06, and the Imagyn Medical Technologies Inc. *isostar* model IS-12501. The ^{103}Pd sources included are the Theragenics Corporation model 200 and NASI model MED3633. The AAPM recommends that the revised dose-calculation protocol and revised source-specific dose-rate distributions be adopted by all end users for clinical treatment planning of low energy brachytherapy interstitial sources. Depending upon the dose-calculation protocol and parameters currently used by individual physicists, adoption of this protocol may result in changes to patient dose calculations. These changes should be carefully evaluated and

reviewed with the radiation oncologist preceding implementation of the current protocol. © *2004 American Association of Physicists in Medicine.* [DOI: 10.1118/1.1646040]

Key words: TG-43, brachytherapy dosimetry protocol, TLD dosimetry, Monte Carlo calculations, ^{125}I, ^{103}Pd

TABLE OF CONTENTS

TG-43 were as large as 17% for some sources. These changes have been exhaustively reviewed by the physics community and are generally accepted. Most treatment planning software vendors have implemented the TG-43 formalism and the recommended dosimetry parameters in their systems. LiF TLD dose measurements and Monte Carlo dose calculations have largely replaced the semi-empirical dose-calculation models of the past.

Since publication of the TG-43 protocol over nine years ago, significant advances have taken place in the field of permanent source implantation and brachytherapy dosimetry. To accommodate these advances, the AAPM deemed it necessary to update this protocol for the following reasons:

(a) To eliminate minor inconsistencies and omissions in the original TG-43 formalism and its implementation.[4–6]
(b) To incorporate subsequent AAPM recommendations, addressing requirements for acquisition of dosimetry data as well as clinical implementation.[7] These recommendations, e.g., elimination of A_{app} (see Appendix E) and description of minimum standards for dosimetric characterization of low-energy photon-emitting brachytherapy sources,[8,9] needed to be consolidated in one convenient document.
(c) To critically reassess published brachytherapy dosimetry data for the ^{125}I and ^{103}Pd source models introduced both prior and subsequent to publication of the TG-43 protocol in 1995, and to recommend consensus datasets where appropriate.
(d) To develop guidelines for the determination of reference-quality dose distributions by both experimental and Monte Carlo methods, and to promote consistency in derivation of parameters used in TG-43 formalism.

Updated tables of TG-43 parameters are necessary and timely to accommodate the ~20 new low-energy interstitial brachytherapy source models that have been introduced to the market since publication of TG-43 in 1995. These commercial developments are due mostly to the rapid increase in utilization of permanent prostate brachytherapy. Some of these new brachytherapy sources were introduced into clinical practice without thorough scientific evaluation of the necessary dosimetric parameters. The AAPM addressed this issue in 1998, recommending that at least one experimental and one Monte Carlo determination of the TG-43 dosimetry parameters be published in the peer-reviewed literature before using new low-energy photon-emitting sources (those with average photon energies less than 50 keV) in routine clinical practice.[9] Thus, many source models are supported by multiple dosimetry datasets based upon a variety of basic dosimetry techniques. This confronts the clinical physicist with the problem of critically evaluating and selecting an appropriate dataset for clinical use. To address this problem, this protocol presents a critical review of dosimetry data for eight ^{125}I and ^{103}Pd source models which satisfied the aforementioned criteria as of July 15, 2001, including the three low-energy source models included in the original TG-43 protocol. The present protocol (TG-43U1) recommends a single, consensus dataset for each source model from which the 1D and 2D dose-rate distribution can be reconstructed. [This protocol was prepared by the AAPM Low-energy Interstitial Brachytherapy Dosimetry subcommittee, now the Photon-Emitting Brachytherapy Dosimetry subcommittee (Chair, Jeffrey F. Williamson) of the AAPM Radiation Therapy Committee. This protocol has been reviewed and approved by the AAPM Radiation Therapy Committee and AAPM Science Council, and represents the current recommendations of the AAPM on this subject.] Finally, methodological guidelines are presented for physicist-investigators aiming to obtain dosimetry parameters for brachytherapy sources using calculative methods or experimental techniques.

Although many of the principles and the changes in methodology might apply, beta- or neutron-emitting sources such as ^{90}Sr, ^{32}P or ^{252}Cf are not considered in this protocol. A further update of this protocol is anticipated to provide consensus, single source dose distributions and dosimetry parameters for high-energy photon-emitting (e.g. ^{192}Ir and ^{137}Cs) sources, and to generate consensus data for new low-energy photon sources that are not included in this report, yet meet the AAPM prerequisites and are posted on the AAPM/RPC Seed Registry website[10] as of December 1, 2003:

(1) Amersham Health, OncoSeed model 6733 ^{125}I,
(2) Best Medical model 2335 ^{103}Pd,
(3) Draximage Inc., BrachySeed model LS-1 ^{125}I,
(4) IBt, Intersource-125 model 1251L ^{125}I,
(5) IBt, Intersource-103 model 1031L ^{103}Pd,
(6) Implant Sciences Corp. I-Plant model 3500 ^{125}I,
(7) IsoAid, Advantage model 1A1-125A ^{125}I,
(8) Mills Biopharmaceuticals Inc., ProstaSeed model SL/SH-125 ^{125}I,
(9) Nucletron Corp., selectSeed model 130.002 ^{125}I, and
(10) SourceTech Medical, ^{125}Implant model STM1251 ^{125}I.

As indicated in the Table of Contents, this protocol is divided into various sections. Clinical medical physicists should pay special attention to Secs. III–VI due to dosimetry formalism and clinical implementation recommendations presented herein. Section II updates the clinical rationale for accurate dosimetry. The origin of consensus datasets for eight seed models is presented in Appendix A. Dosimetry investigators will find useful the detailed recommendations presented in Secs. IV and V. The description of the NIST calibration scheme is presented in Appendix B. Manufacturers of brachytherapy treatment planning software will find new recommendations in Secs. II, IV, VI, and Appendixes C–E.

II. CLINICAL RATIONALE FOR ACCURATE DOSIMETRY

While low-energy, photon-emitting brachytherapy sources have been used to treat cancers involving a variety of anatomical sites, including eye plaque therapy for choroidal

melanoma and permanent lung implants,[11,12] their most frequent indication today is for the treatment of prostate cancer.[13]

A. General 2D formalism

The general, two-dimensional (2D) dose-rate equation from the 1995 TG-43 protocol is retained,

$$\dot{D}(r,\theta)=S_K\cdot\Lambda\cdot\frac{G_L(r,\theta)}{G_L(r_0,\theta_0)}\cdot g_L(r)\cdot F(r,\theta), \quad (1)$$

where r denotes the distance (in centimeters) from the center of the active source to the point of interest, r_0 denotes the reference distance which is specified to be 1 cm in this protocol, and θ denotes the polar angle specifying the point-of-interest, $P(r,\theta)$, relative to the source longitudinal axis. The reference angle, θ_0, defines the source transverse plane, and is specified to be 90° or $\pi/2$ radians (Fig. 1).

In clinical practice, source position and orientation are identified by means of radio-opaque markers. Generally, these markers are positioned symmetrically within the source capsule such that the marker, the radioactivity distribution, and the capsule have the same geometric center on the symmetry axis of the source. Thus, determination of the location of the radioisotope distribution is based upon identification of the radio-opaque markers. All sources discussed in this document can be accurately represented by a capsule and radio-opaque markers that are symmetric with respect to the transverse plane, which by definition bisects the active source and specifies the origin of the dose-calculation formalism. However, Eq. (1) can accommodate sources that are asymmetric with respect to the transverse plane. For sources that exhibit all of the following characteristics: (i) the radioactivity distribution is clearly asymmetric with respect to the planes bisecting the capsule or marker; (ii) the extent of asymmetry is known *a priori* or can be measured via imaging; and (iii) the source orientation can be determined under clinical implant circumstances (e.g., via CT or radiography), then the source coordinate system origin should be positioned at the geometric center of the radionuclide distribution (as determined using positioning information obtained from the markers), not the geometric center of the exterior surface of the capsule or marker. If radio-opaque markers do not facilitate identification of source orientation and the asymmetrical distribution under clinical circumstances, then the geometric center of the source must be presumed to reside at the radio-opaque marker centroid as is conventionally performed.

The quantities used in Eq. (1) are defined and discussed later. This formalism applies to sources with cylindrically symmetric dose distributions with respect to the source longitudinal axis. In addition, the consensus datasets presented in Sec. IV B assume that dose distributions are symmetric with respect to the transverse plane, i.e., that radioactivity distributions to either side of the transverse plane are mirror images of one another. However, this formalism is readily generalized to accommodate sources that are not symmetric with respect to the transverse plane.

Equation (1) includes additional notation compared with the corresponding equation in the original TG-43 formalism, namely the subscript "L" has been added to denote the line source approximation used for the geometry function (Sec. III A 3). For evaluation of dose rates at small and large distances, the reader is referred to Appendix C.

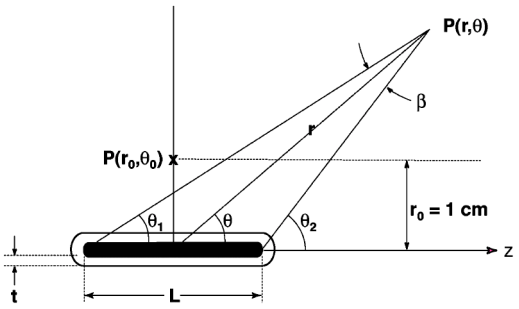

FIG. 1. Coordinate system used for brachytherapy dosimetry calculations.

1. Air-kerma strength

This protocol proposes minor revisions to the definition of air-kerma strength, S_K, which was first introduced by the AAPM TG-32 report in 1987.[22] Air-kerma strength has units of $\mu\text{Gy m}^2\text{ h}^{-1}$ and is numerically identical to the quantity Reference Air Kerma Rate recommended by ICRU 38 and ICRU 60.[23,24] For convenience, these unit combinations are denoted by the symbol U where $1\text{ U}=1\ \mu\text{Gy m}^2\text{ h}^{-1}=1\text{ cGy cm}^2\text{ h}^{-1}$.

Air-kerma strength, S_K, is the air-kerma rate, $\dot{K}_\delta(d)$, *in vacuo* and due to photons of energy greater than δ, at distance d, multiplied by the square of this distance, d^2,

$$S_K=\dot{K}_\delta(d)d^2. \quad (2)$$

The quantity d is the distance from the source center to the point of $\dot{K}_\delta(d)$ specification (usually but not necessarily associated with the point of measurement) which should be located on the transverse plane of the source. The distance d can be any distance that is large relative to the maximum linear dimension of the radioactivity distribution so that S_K is independent of d. $\dot{K}_\delta(d)$ is usually inferred from transverse-plane air-kerma rate measurements performed in a free-air geometry at distances large in relation to the maximum linear dimensions of the detector and source, typically of the order of 1 meter. The qualification "*in vacuo*" means that the measurements should be corrected for photon attenuation and scattering in air and any other medium interposed between the source and detector, as well as photon scattering from any nearby objects including walls, floors, and ceilings. Of course, air-kerma rate may also be calculated to subvert some of the limitations imposed on practical measurements.[25] The energy cutoff, δ, is intended to exclude low-energy or contaminant photons (e.g., characteristic x-rays originating in the outer layers of steel or titanium source cladding) that increase $\dot{K}_\delta(d)$ without contributing significantly to dose at distances greater than 0.1 cm in tissue. The value of δ is typically 5 keV for low-energy photon-emitting brachytherapy sources, and is dependent on the application.

In summary, the present definition of S_K differs in two important ways from the original 1987 AAPM definition. First, the original AAPM definition of S_K did not allow for a low-energy cutoff. Subsequent experience using free-air chambers as primary S_K standards clearly indicates that failure to exclude nonpenetrating radiations greatly increases measurement uncertainty and invalidates theoretical dosimetry models. Second, the conditions that should prevail in an experimental determination of S_K are now explicitly stated.

2. Dose-rate constant

The definition of the dose-rate constant in water, Λ, is unchanged from the original TG-43 protocol: it is the ratio of dose rate at the reference position, $P(r_0,\theta_0)$, and S_K. Λ has units of $\mathrm{cGy\,h^{-1}\,U^{-1}}$ which reduces to $\mathrm{cm^{-2}}$,

$$\Lambda = \frac{\dot{D}(r_0,\theta_0)}{S_K}. \tag{3}$$

The dose-rate constant depends on both the radionuclide and source model, and is influenced by both the source internal design and the experimental methodology used by the primary standard to realize S_K.

In 1999, a notation was introduced, $\Lambda_{nnD,PqqS}$, to identify both the dose-rate measurements or calculations used to determine $\dot{D}(r_0,\theta_0)$ and the calibration standard to which this dose rate was normalized. The subscript "*D*" denotes *reference dose rate*, "*nn*" denotes the year in which this reference dose rate was published (either measurement or calculation), "*P*" denotes the *provider* or origin of the source strength standard (e.g., *P*="*N*" for NIST, or *P*="*T*" for the in-house calibration-standard of Theragenics Corporation), "*qq*" denotes the year in which this source strength standard was implemented, and the "*S*" subscript denotes the word *standard*.[7] For example, $\Lambda_{97D,N99S}$ indicates a dose-rate constant determined from dosimetry measurements published in 1997 and normalized to an S_K traceable to the 1999 NIST standard. Additional notation may also be utilized such as ${}^{6702}_{\mathrm{TLD}}\Lambda_{97D,N85S}$ for the dose-rate constant for the model 6702 source published in 1997 using TLDs and the 1985 NIST standard. These notations are useful for comparing results from multiple investigators, and readily highlight features such as utilization of the calibration procedure and whether or not influence of titanium *K*-shell x rays is included.

3. Geometry function

Within the context of clinical brachytherapy dose calculations, the purpose of the geometry function is to improve the accuracy with which dose rates can be estimated by interpolation from data tabulated at discrete points. Physically, the geometry function neglects scattering and attenuation, and provides an effective inverse square-law correction based upon an *approximate model* of the spatial distribution of radioactivity within the source. Because the geometry function is used only to interpolate between tabulated dose-rate values at defined points, highly simplistic approximations yield sufficient accuracy for treatment planning. This protocol recommends use of point- and line-source models giving rise to the following geometry functions:

$$G_P(r,\theta) = r^{-2} \quad \text{point-source approximation,}$$
$$G_L(r,\theta) = \begin{cases} \dfrac{\beta}{Lr\sin\theta} & \text{if} \quad \theta \neq 0^\circ \\ (r^2 - L^2/4)^{-1} & \text{if} \quad \theta = 0^\circ \end{cases} \quad \text{line-source approximation,} \tag{4}$$

where β is the angle, in radians, subtended by the tips of the hypothetical line source with respect to the calculation point, $P(r,\theta)$.

In principle, either the point-source or line-source models may be consistently implemented in both the 1D and 2D versions of the TG-43 formalism. In this case, the word "consistently" means that the geometry function used for derivation of dose rates from TG-43 parameters should be identical to that used to prepare the radial dose function and 2D anisotropy function data, including use of the same active length, L, used in $G(r,\theta)$. Under these conditions, TG-43 dose calculations will reproduce exactly the measured or Monte Carlo-derived dose rates from which $g(r)$ and $F(r,\theta)$ tables were derived. This protocol recommends consistent use of the line-source geometry function for evaluation of 2D dose distributions, and use of either point- or line-source geometry functions for evaluations of 1D dose distributions. Use of such simple functions is warranted since their purpose is to facilitate interpolation between tabulated data entries for duplication of the original dosimetry results.

In the case where the radioactivity is distributed over a right-cylindrical volume or annulus, this protocol recommends taking active length to be the length of this cylinder. For brachytherapy sources containing uniformly spaced multiple radioactive components, L should be taken as the effective length, L_{eff}, given by

$$L_{\mathrm{eff}} = \Delta S \times N, \tag{5}$$

where N represents the number of discrete pellets contained in the source with a nominal pellet center-to-center spacing ΔS. If L_{eff} is greater than the physical length of the source capsule (usually $\sim$4.5 mm), the maximum separation (distance between proximal and distal aspects of the activity distribution) should be used as the active length, L. This tech-

nique avoids singularities in evaluating $G(r,\theta)$ for points of interest in tissue which are located on the hypothetical line source just beyond the tip and end of the physical source.

More complex forms of the geometry function have a role in accurately estimating dose at small distances outside the tabulated data range, i.e., extrapolating $g(r)$ and $F(r,\theta)$ to small distances.[26,27] Use of such expressions is permitted. However, most commercial brachytherapy treatment planning systems support only point- or line-source geometry functions. Therefore, it is the responsibility of the physicist to transform the tabulated TG-43 parameters given in this protocol, which are based upon point- and line-source approximations, to a format consistent with more complex geometry functions that may be available on their treatment planning systems.[28–30]

4. Radial dose function

The radial dose function, $g_X(r)$, accounts for dose fall-off on the transverse-plane due to photon scattering and attenuation, i.e., excluding fall-off included by the geometry function. $g_X(r)$ is defined by Eq. (6), and is equal to unity at $r_0 = 1$ cm.

$$g_X(r) = \frac{\dot{D}(r,\theta_0)}{\dot{D}(r_0,\theta_0)} \frac{G_X(r_0\theta_0)}{G_X(r,\theta_0)}. \tag{6}$$

The revised dose-calculation formalism has added the subscript "X" to the radial dose function and geometry function to indicate whether a point-source, "P," or line-source, "L," geometry function was used in transforming the data. Consequently, this protocol presents tables of both $g_P(r)$ and $g_L(r)$ values.

Equation (7) corrects a typographical error in the original TG-43 protocol.[31] While table lookup via linear interpolation or any appropriate mathematical model fit to the data may be used to evaluate $g_X(r)$, some commercial treatment planning systems currently accommodate a fifth-order polynomial fit to the tabulated $g(r)$ data. Since this type of polynomial fit may produce erroneous results with large errors outside the radial range used to determine the fit, alternate fitting equations have been proposed which are less susceptible to this effect,[32]

$$g_X(r) = a_0 + a_1 r + a_2 r^2 + a_3 r^3 + a_4 r^4 + a_5 r^5. \tag{7}$$

Parameters a_0 through a_5 should be determined so that they fit the data within $\pm 2\%$. Also, the radial range over which the fit meets this specification should be clearly specified.

5. 2D anisotropy function

The 2D anisotropy function, $F(r,\theta)$, is defined as

$$F(r,\theta) = \frac{\dot{D}(r,\theta)}{\dot{D}(r,\theta_0)} \frac{G_L(r,\theta_0)}{G_L(r,\theta)}. \tag{8}$$

Other than inclusion of the subscript L, this definition is identical to the original TG-43 definition.[1] The 2D anisotropy function describes the variation in dose as a function of polar angle relative to the transverse plane. While $F(r,\theta)$ on the transverse plane is defined as unity, the value of $F(r,\theta)$ off the transverse plane typically decreases as (i) r decreases, (ii) as θ approaches 0° or 180°, (iii) as encapsulation thickness increases, and (iv) as photon energy decreases. However, $F(r,\theta)$ may exceed unity at $|\theta - 90°| > \pm \arcsin(L/2r)$ for right-cylinder sources coated with low-energy photon emitters due to screening of photons by the active element at angles towards the transverse plane.

As stated earlier, the active length, L, used to evaluate $G_L(r,\theta)$ in Eq. (4) shall be the same L used to extract $g_L(r)$ and $F(r,\theta)$ from dose distributions via Eqs. (6) and (8), respectively. Otherwise, significant errors in dosimetry results at small distances may arise. For example, at $r = 0.5$ cm, a change in L from 3 to 5 mm results in a 5% change in $G_L(r,\theta_0)$.

B. General 1D formalism

While a 1D isotropic point-source approximation [Eq. (9)] only approximates the true complex 2D dose distribution, it

lization of the 1D dosimetry formalism presented in Eq. (12), or other formalisms that inconsistently apply the geometry function, *are not recommended*.

1. 1D anisotropy function

The 1D anisotropy function, $\phi_{an}(r)$, is identical to the anisotropy factor defined by the original TG-43 protocol. At a given radial distance, $\phi_{an}(r)$ is the ratio of the solid angle-weighted dose rate, averaged over the entire 4π steradian space, to the dose rate at the same distance r on the transverse plane, see Eq. (13),

$$\phi_{an}(r)=\frac{\int_0^{\pi}\dot{D}(r,\theta)\sin(\theta)d\theta}{2\dot{D}(r,\theta_0)}. \tag{13}$$

Note that one should integrate dose rate, not the values of the 2D anisotropy function to arrive at $\phi_{an}(r)$.

With consistent use of the geometry function, both Eqs. (10) and (11) will exactly reproduce the solid-angle weighted dose rate at a given r. Of the two, Eq. (11) is recommended because the line-source geometry function will provide more accurate interpolation and extrapolation at small distances. The accuracy achievable using the 1D formalism for prostate implants was reported by Lindsay *et al.*,[33] and Corbett *et al.*[34]

For brachytherapy treatment planning systems that do not permit entry of $\phi_{an}(r)$, Eqs. (10) or (11) can still be implemented by carefully modifying $g_X(r)$ to include $\phi_{an}(r)$ as shown in Eq. (14). These modified dosimetry parameters, $g'(r)$ and $\overline{\phi}'_{an}$, are defined as

$$g'(r)=g_X(r)\cdot\phi_{an}(r),$$
$$\overline{\phi}'_{an}=1. \tag{14}$$

While TG-43 introduced the anisotropy constant, $\overline{\phi}_{an}$, LIBD no longer recommends its use. This is discussed in greater detail in Appendix D.

IV. CONSENSUS DATASETS FOR CLINICAL IMPLEMENTATION

The ^{125}I and ^{103}Pd source models reviewed in this protocol (Fig. 2) satisfied the AAPM recommendations that comprehensive (2D) reference-quality dose-rate distribution data be accepted for publication by a peer-reviewed scientific journal on or before July 15, 2001. Appropriate publications can report either Monte Carlo, or experimentally derived TG-43 dosimetry parameters. As many as 12 sets of independently published data per source model were evaluated during preparation for this report. For each source model, a single consensus dataset was derived from multiple published datasets according to the following methodology.[35] If items essential to critical evaluation were omitted, the authors were contacted for information or clarification.

(a) The peer-reviewed literature was examined to identify candidate dose distributions for each source model derived either from experimental measurements or Monte Carlo simulations. Experimentally determined values for the dose-rate constant ($_{EXP}\Lambda$) were averaged. Separately, Λ values obtained using Monte Carlo techniques ($_{MC}\Lambda$) were averaged. The consensus value recommended in this protocol ($_{CON}\Lambda$) is the equally weighted average of the separately averaged experimental and Monte Carlo Λ values. In cases where there is only one experimental result and one Monte Carlo result: $_{CON}\Lambda=[_{EXP}\Lambda+_{MC}\Lambda]/2$.

(b) Each candidate dataset was examined separately and eliminated from consideration if it was determined to have a problem, e.g., data inconsistency. Corrections for use of a nonliquid water measurement phantom were applied if not included in the original investigators' analysis.

(c) For the 2D anisotropy function, $F(r,\theta)$, and the radial dose function, $g(r)$, all candidate datasets for a given source model were transformed using identical line-source geometry functions to permit fair comparison. The radial dose function was corrected for nonliquid water measurement medium if necessary. Assuming that the different datasets agreed within experimental uncertainties, the consensus data were defined as the ideal candidate dataset having the highest resolution, covering the largest distance range, and having the highest degree of smoothness. For most source models examined in this protocol, the consensus $F(r,\theta)$ and $g(r)$ data, $_{CON}F(r,\theta)$ and $_{CON}g(r)$, were taken from the transformed Monte Carlo dataset.

(d) A few entries in the tabulated consensus datasets were taken from the nonideal candidate dataset(s) to cover a larger range of distances and angles. These data were *italicized* to indicate that they were not directly confirmed by other measurements or calculations.

(e) The 1D anisotropy function, $\phi_{an}(r)$, was derived using numerical integration of the dose rate, as calculated from $_{CON}F(r,\theta)$ dataset, with respect to solid angle. Use of the anisotropy constant, $\overline{\phi}_{an}$, is discouraged as discussed in Appendix D.

(f) When scientifically justified for a given source model, exceptions or modifications to these rules were made, and are described later. For example, if the datasets were too noisy, they were rejected.

(g) Following tabulation of $g(r)$ and $F(r,\theta)$ for all eight source models, overly dense datasets were downsampled to permit reasonable comparisons. Removal of a dataset point was deemed reasonable if linear interpolation using adjacent points resulted in a difference no larger than $\pm 2\%$ of the dataset point in question. Similarly, because the various authors used different table grids, it was necessary to interpolate some of the data into the common mesh selected for presenting all eight datasets. Linear–linear interpolation was used for $F(r,\theta)$ datasets, and log-linear interpolation was used for $g(r)$ datasets. Interpolated data are indicated by **boldface**.

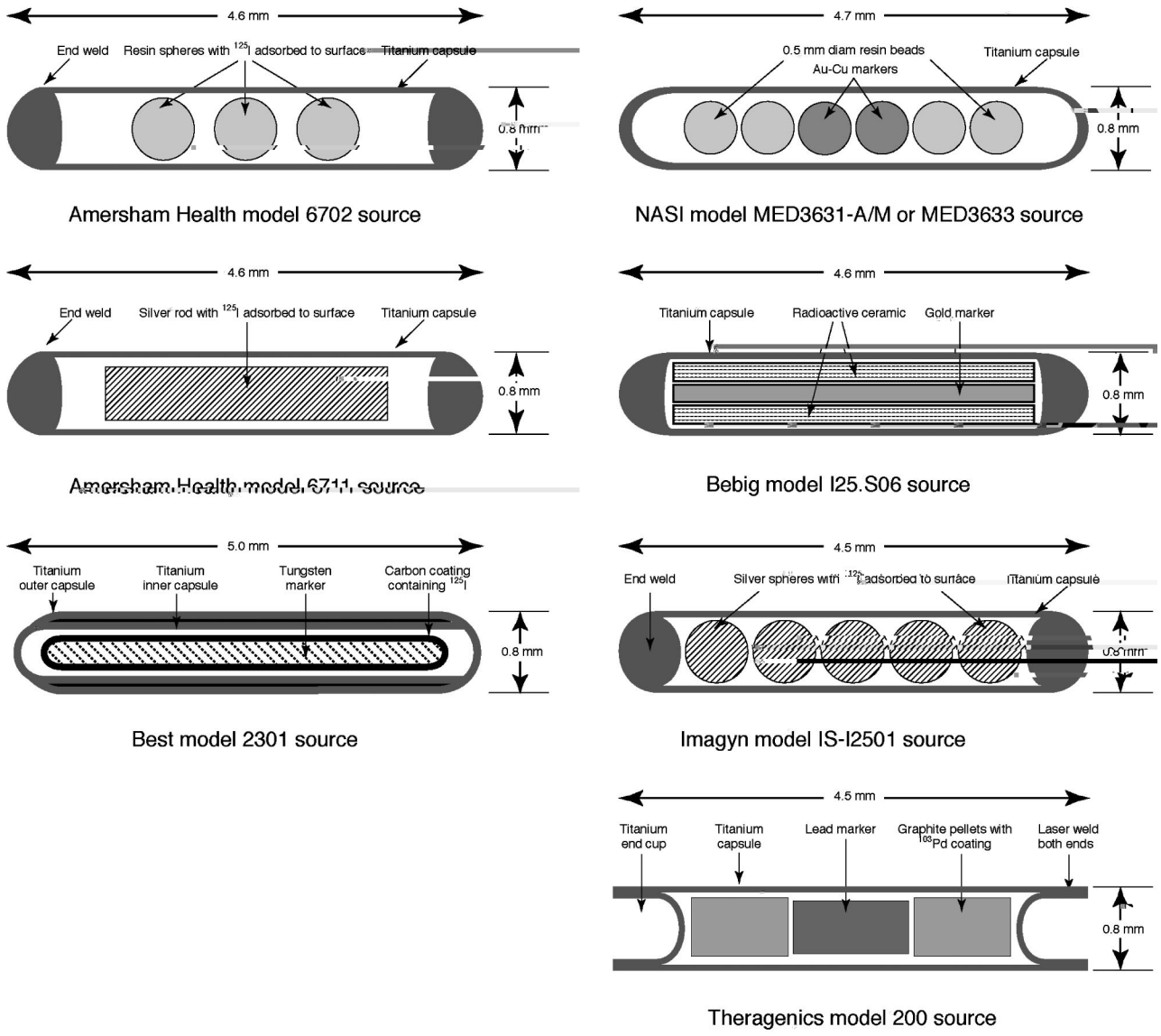

FIG. 2. Brachytherapy seeds examined in this report: (a) Amersham model 6702 source, (b) Amersham model 6711 source, (c) Best model 2301 source, (d) NASI model MED3631-A/M or MED3633 source, (e) Bebig/Theragenics Corp. model I25.S06 source, (f) Imagyn model IS-12501 source, and (g) Theragenics Corp. model 200 source. The titanium capsule is 0.06 mm thick for the Amersham and Theragenics seeds, while each capsule of the Best seed is 0.04 mm thick. The capsule thickness of the remaining seeds is 0.05 mm.

The details used to evaluate dosimetry parameters for each source were the following:

(1) internal source geometry and a description of the source,
(2) review of the pertinent literature for the source,
(3) correction coefficients for 1999 anomaly in NIST air-kerma strength measurements (if applicable),
(4) solid water-to-liquid water corrections,
(5) experimental method used, TLD or diode,
(6) active length assumed for the geometry function line-source approximation,
(7) name and version of the Monte Carlo transport code,
(8) cross-section library used by Monte Carlo simulation,
(9) Monte Carlo estimator used to score kerma or dose, and
(10) agreement between Monte Carlo calculations and experimental measurement.

A. Source geometry variations

Source geometry and internal construction are highly manufacturer specific. Source models vary from one another with regard to weld thickness and type, radioactivity carrier construction, presence of radio-opaque material with sharp or rounded edges, the presence of silver (which produces characteristic x rays that modify the photon spectrum), and capsule wall thickness. All of these properties can affect the dosimetric characteristics of the source. Radioactive carriers may consist of a radio-transparent matrix, a radio-opaque object coated with radioactivity, or a radio-transparent matrix with highly attenuating radioactive coating. For example, the Amersham model 6702 and NASI model 3631-A/M sources utilize spherical resin carriers coated or impregnated with radioactivity. The number of spheres varies from 3 or more

per source. Other sources, such as the Amersham model 6711, utilize a silver rod carrier. The amount of silver, or the length of silver rod, varies by the source model. Graphite pellets are also used. For example, in the Theragenics Corporation model 200 ^{103}Pd source, the pellets are coated with a mixture of radioactive and nonradioactive palladium.

All ^{125}I and ^{103}Pd source models, except for the now-obsolete model 6702 source, contain some type of radio-opaque marker to facilitate radiographic localization. For example, the graphite pellets of the Theragenics Corporation source are separated by a cylindrical lead marker. Beside the obvious dependence of photon spectrum on the radioisotope used, the backing material (e.g., the radio-opaque marker) may further perturb the spectrum. For the sources containing ^{125}I deposited on silver, the resultant silver x rays significantly modify the effective photon spectrum. These source construction features influence the resultant dose rate distribution and the TG-43 dosimetry parameters to varying degrees. Accurate knowledge of internal source geometry and construction details is especially important for Monte Carlo modeling. Individual sources are briefly described later. References describing each source and the TG-43 parameters are given in each section. While Sec. III presented the dosimetry formalism, its applicability to the derivation of consensus datasets is given later. A detailed description for seed models is provided in Appendix A.

B. General discussion of TG-43 dosimetry parameters

1. Air-kerma strength standards

The NIST Wide-Angle Free-Air Chamber or WAFAC-based primary standard became available in 1998, and was used to standardize the ^{125}I sources then available (models 6702, 6711, and MED3631-A/M). For a more detailed discussion of the NIST air-kerma strength standards, including those based on the Ritz free-air chamber (1985) and WAFAC (1999), see Appendix B. The WAFAC standard shifted for unknown reasons in 1999, and was corrected in the first half of 2000. For those sources available in 1998, the 1998 and 2000 WAFAC measurements agreed within estimated measurement uncertainty. Following restoration of the WAFAC to its 1998 sensitivity in 2000, all sources initially standardized against WAFAC measurements performed in 1999, and the model 3631-A/M source, which had renormalized its stated strength against the WAFAC in 1999, had to be standardized against the corrected WAFAC measurements. To implement these corrections, five sources of each type were calibrated using the NIST WAFAC and then sent to both the accredited dosimetry calibration laboratories (ADCLs) and the manufacturer for intercomparisons with their transfer standards. The AAPM Calibration Laboratory Accreditation subcommittee, in conjunction with NIST, selected the NIST WAFAC calibration date as the reference date for each source model, converting stated source strengths to the NIST WAFAC 1999 standard as corrected in 2000. This date, as described on ADCL calibration reports as the vendor traceability date, gives the date of the WAFAC calibration measurements to which the certified calibration is traceable. All vendors discussed in this protocol have agreed to accept

TABLE I. NIST standard WAFAC calibration dates for air kerma strength for each manufacturer, and dose rate constant values. Note that for a given source type, the % change in Λ from the 1999 value is not necessarily equal to the average % change in air-kerma strength due the 1999 NIST WAFAC anomaly because some of the Λ values were calculated based on air-kerma strength measurements of a single seed.

Manufacturer and source type		NIST date used by ADCL and NIST as standard	${}_{\mathrm{CON}}\Lambda$ $[\mathrm{cGy}\cdot\mathrm{h}^{-1}\cdot\mathrm{U}^{-1}]$	% difference in Λ from 1999 value
Amersham 6702	^{125}I	April 15, 1998	1.036	N/A
Amersham 6711	^{125}I	April 15, 1998	0.965	N/A
Best Industries 2301	^{125}I	August 18, 2000	1.018	+3.3%
NASI MED3631-A/M	^{125}I	June 30, 2001	1.036	+1.0%
Bebig/Theragenics I25.S06	^{125}I	January 27, 2001	1.012	+2.2%
Imagyn IS-12501	^{125}I	October 21, 2000	0.940	+3.5%
Theragenics 200	^{103}Pd	July 8, 2000	0.686	+4.0%
NASI MED3633	^{103}Pd	April 23, 2001	0.688	+4.3%

small manufacturing changes on the uncertainty of calculated dose-rate distributions. Therefore, the use of Monte Carlo values without confirmation by experimental studies is highly undesirable. Drawbacks of TLD dosimetry include (a) limited precision of repeated readings and spatial resolution; (b) a large and somewhat uncertain relative energy response correction; (c) failure of most investigators to monitor or control the composition of the measurement medium. For these reasons, the LIBD recommends using an equally weighted average of the average measured (e.g., using TLDs) and average calculated (e.g., Monte Carlo derived) values (see Table I for each source) since the two recommended dosimetry characterization techniques have complementary strengths and limitations.

The values in Table I are the average of experimental and Monte Carlo results, e.g., ${}_{\mathrm{CON}}\Lambda$, for each source model. Experimental results normalized to the 1985 Loftus NIST standard have been corrected to agree with the NIST WAFAC 1999 standard as corrected in 2000.[158] In those cases where the authors did not correct for differences between Solid Water™ and liquid water, corrections were applied based on Williamson's Monte Carlo calculations.[37] Also, a number of the cited experimental dosimetry papers published dose-rate constants are normalized to WAFAC measurements performed in 1999. In these cases, appropriate corrections were made to the published dose-rate constant values.

3. Radial dose function

For each source, Monte Carlo values of $g(r)$ were graphically compared with experimental values. A comparison of the Monte Carlo and experimental $g(r)$ results were expected to show an average agreement of $\pm 10\%$. While the observed differences were typically $<5\%$ for $r \leqslant 5$ cm, systematic differences as large as 10% were observed due to use of outdated Monte Carlo cross-section libraries. Experimental values are difficult to measure at $r<1$ cm, but Monte Carlo calculation of dose rate values are often available at smaller distances. In each case, the most complete dataset (typically Monte Carlo values) was used since values were more readily available over a larger range of distances (especially at clinically significant distances closer than 1 cm) than provided by experimental measurements. The ${}_{\mathrm{CON}}g(r)$ data for all ^{125}I and ^{103}Pd sources and for line- and point-source geometry functions are presented in Tables II and III, respectively. Details used in the determination of $g(r)$ for each source model are provided in Appendix A.

4. 2D anisotropy function

Because Monte Carlo based datasets generally have superior smoothness, spatial and angular resolution, and distance range, all anisotropy functions recommended in this protocol are derived from Monte Carlo results which have been validated by comparison to less complete experimental datasets. A graphical comparison of datasets was performed, and the agreement between the Monte Carlo datasets and the experimental datasets was again expected to be $\pm 10\%$. For $\theta > 30°$, observed differences between the datasets were typically $<5\%$ with a maximum of about 9%. For $\theta \leqslant 30°$, differences were larger (typically $\sim 10\%$ with maximum $\sim 17\%$), and are attributed to volume averaging and the high-dose-rate gradient near the source longitudinal-axis as well as uncertainties in the source geometry assumed by Monte Carlo simulations. Tables IV–XI present the $F(r,\theta)$ and $\phi_{\mathrm{an}}(r)$ data for the sources examined herein.

C. Uncertainty analysis

Most of the experimental and computational investigations, especially those published prior to 1999, failed to include a rigorous uncertainty analysis. Thus, the AAPM recommends that the generic uncertainty analysis described by Table XII, based on the best estimate of uncertainty of the measured dose rate constants used to compute the ${}_{\mathrm{CON}}\Lambda$ values recommended by this report, should be included henceforth. In the future, the AAPM recommends that dosimetry investigators include rigorous uncertainty analyses, specific to their methodology employed, in their published articles. Table XII, based on the works of Gearheart *et al.*[38] and Nath and Yue,[39] assigns a total 1σ uncertainty of 8%–9% to TLD measurements of dose-rate constant and an uncertainty of 5%–7% to measurements of relative quantities.

Based on results of Monroe and Williamson,[37,40] purely Monte Carlo estimates of the transverse-axis dose-rate per unit air-kerma strength typically have uncertainties of 2%–3% at 1 cm and 3%–5% at 5 cm, depending on the type and magnitude of internal seed geometric uncertainties. Since relatively little has been published on estimation of

TABLE II. Consensus $g(r)$ values for six ^{125}I sources. Interpolated data are boldface, and italicized data are nonconsensus data obtained from candidate datasets.

r [cm]						

systematic (type B) uncertainties of Monte Carlo-based dose estimation, the following sections apply the principles of uncertainty analysis, as outlined in NIST Technical Note 1297,[41] to estimation of total uncertainty of Monte Carlo dose-rate constants, ${}_{\mathrm{MC}}\Lambda$, Monte Carlo radial dose functions ${}_{\mathrm{MC}}g(r)$, consensus dose-rate constants, ${}_{\mathrm{CON}}\Lambda$, and absolute transverse-axis dose as evaluated by the dosimetric parameters recommended by this report.

NIST Report 1297 recommends using the Law of Propagation of Uncertainty (LPU) to estimate the uncertainty of a quantity y, that has a functional dependence on measured or estimated quantities $x_1,\ldots,x_N$, as follows:

$$y=f(x_1,\ldots,x_N),$$
$$\sigma_y^2=\sum_{i=1}^{N}\left(\frac{\partial f}{\partial x_i}\right)^2\sigma_{x_i}^2+2\sum_{i=1}^{N-1}\sum_{j=i+1}^{N}\frac{\partial f}{\partial x_i}\frac{\partial f}{\partial x_j}\sigma_{x_i,x_j}, \tag{15}$$

where σ_{x_i,x_j} (assumed zero here) represents the covariance of the two variables. For each dosimetric quantity, $Y(\Lambda,g(r)$, etc.), the total percent uncertainty, $\%\sigma_Y$, is considered to be composed of three sources: type B uncertainty due to uncertainty of the underlying cross sections, $\%\sigma_{Y|\mu}$; type B uncertainties arising from uncertainty of the seed geo-

TABLE IV. $F(r,\theta)$ for Amersham model 6702.

Polar angle θ (degrees)	r [cm]					
	0.5	1	2	3	4	5
0	0.385	0.420	0.493	0.533	0.569	0.589
5	0.413	0.472	0.546	0.586	0.613	0.631
10	0.531	0.584	0.630	0.660	0.681	0.697
15	0.700	0.700	0.719	0.738	0.749	0.758
20	0.788	0.789	0.793	0.805	0.810	0.814
30	0.892	0.888	0.888	0.891	0.892	0.892
40	0.949	0.948	0.944	0.944	0.944	0.944
50	0.977	0.973	0.967	0.967	0.967	0.967
60	0.989	0.985	0.983	0.983	0.983	0.983
70	0.996	0.992	0.990	0.990	0.990	0.990
80	1.000	0.998	0.998	0.998	0.998	0.998
$\phi_{an}(r)$	0.986	0.960	0.952	0.951	0.954	0.954

TABLE V. $F(r,\theta)$ for Amersham model 6711.

Polar angle θ (degrees)	r [cm]					
	0.5	1	2	3	4	5
0	0.333	0.370	0.442	0.488	0.520	0.550
5	0.400	0.429	0.497	0.535	0.561	0.587
10	0.519	0.537	0.580	0.609	0.630	0.645
20	0.716	0.705	0.727	0.743	0.752	0.760
30	0.846	0.834	0.842	0.846	0.848	0.852
40	0.926	0.925	0.926	0.926	0.928	0.928
50	0.972	0.972	0.970	0.969	0.969	0.969
60	0.991	0.991	0.987	0.987	0.987	0.987
70	0.996	0.996	0.996	0.995	0.995	0.995
80	1.000	0.998	0.998	0.998	0.998	0.998
$\phi_{an}(r)$	0.986	0.960	0.952	0.951	0.954	0.954

488 0 0 5.488 140.018 566.931.7(488 888 8.318 Tm(ABLE)Tj 7.81.77(0.7.982 149.08447 126.398.7(0.587)]TJ
20
0.14 138447

TABLE VII. $F(r,\theta)$ for NASI model MED3631-A/M.

Polar angle θ (degrees)	r [cm]					
	0.25	0.5	1	2	5	10
0	1.038	0.690	0.702	0.667	0.718	0.771
10	0.984	0.700	0.662	0.676	0.728	0.758
20	0.916	0.761	0.747	0.764	0.794	0.815
30	0.928	0.854	0.846	0.852	0.871	0.878
40	0.941	0.909	0.906	0.909	0.918	0.914
50	0.962	0.949	0.949	0.950	0.958	0.954
60	0.975	0.975	0.975	0.975	0.983	0.972
70	0.991	0.989	0.992	0.990	0.993	0.989
80	0.999	0.999	1.003	0.996	0.998	0.999
$\phi_{an}(r)$	1.288	1.008	0.952	0.945	0.948	0.948

TABLE VIII. $F(r,\theta)$ for Bebig/Theragenics model I25.S06. Italicized data are nonconsensus data obtained from candidate datasets.

Polar angle θ (degrees)	r [cm]							
	0.25	*0.5*	1	2	3	4	*5*	*7*
0	*0.302*	*0.429*	0.512	0.579	0.610	0.631	*0.649*	*0.684*
5	*0.352*	*0.436*	0.509	0.576	0.610	0.635	*0.651*	*0.689*
10	*0.440*	*0.476*	0.557	0.622	0.651	0.672	*0.689*	*0.721*
20	*0.746*	*0.686*	0.721	0.757	0.771	0.785	*0.790*	*0.807*
30	*0.886*	*0.820*	0.828	0.846	0.857	0.862	*0.867*	*0.874*
40	*0.943*	*0.897*	0.898	0.907	0.908	0.913	*0.918*	*0.912*
50	*0.969*	*0.946*	0.942	0.947	0.944	0.947	*0.949*	*0.946*
60	*0.984*	*0.974*	0.970	0.974	0.967	0.966	*0.967*	*0.976*
70	*0.994*	*0.989*	0.988	0.990	0.984	0.985	*0.987*	*0.994*
80	*0.998*	*0.998*	0.998	1.000	0.994	1.000	*0.993*	*0.999*
$\phi_{an}(r)$	*1.122*	*0.968*	0.939	0.939	0.938	0.940	*0.941*	*0.949*

TABLE IX. $F(r,\theta)$ for Imagyn model IS-12501. Italicized data are nonconsensus data obtained from candidate datasets.

Polar angle θ (degrees)	r [cm]				
	1	2	3	5	7
0	*0.241*	0.337	0.362	0.424	0.454
10	*0.327*	0.399	0.440	0.486	0.510
20	*0.479*	0.532	0.563	0.584	0.581
30	*0.634*	0.663	0.681	0.706	0.700
40	*0.768*	0.775	0.786	0.806	0.776
50	*0.867*	0.870	0.878	0.875	0.849
60	*0.946*	0.944	0.944	0.943	0.913
70	*0.986*	0.985	0.987	0.974	0.955
80	*0.998*	0.994	1.004	0.981	0.956
$\phi_{an}(r)$	*0.867*	0.886	0.894	0.897	0.879

TABLE X. $F(r,\theta)$ for Theragenics Corp. model 200. Italicized data are nonconsensus data obtained from candidate datasets.

Polar angle θ (degrees)	r (cm)								
	0.25	*0.5*	0.75	1	2	3	4	5	*7.5*
0	*0.619*	*0.694*	*0.601*	0.541	0.526	0.504	0.497	0.513	*0.547*
1	*0.617*	*0.689*	*0.597*	0.549	0.492	0.505	0.513	0.533	*0.580*
2	*0.618*	*0.674*	*0.574*	0.534	0.514	0.517	0.524	0.538	*0.568*
3	*0.620*	*0.642*	*0.577*	0.538	0.506	0.509	0.519	0.532	*0.570*
5	*0.617*	*0.600*	*0.540*	0.510	0.499	0.508	0.514	0.531	*0.571*
7	*0.579*	*0.553*	*0.519*	0.498	0.498	0.509	0.521	0.532	*0.568*
10	*0.284*	*0.496*	*0.495*	0.487	0.504	0.519	0.530	0.544	*0.590*
12	*0.191*	*0.466*	*0.486*	0.487	0.512	0.529	0.544	0.555	*0.614*
15	*0.289*	*0.446*	*0.482*	0.490	0.523	0.540	0.556	0.567	*0.614*
20	*0.496*	*0.442*	*0.486*	0.501	0.547	0.568	0.585	0.605	*0.642*
25	*0.655*	*0.497*	*0.524*	0.537	0.582	0.603	0.621	0.640	*0.684*
30	*0.775*	*0.586*	*0.585*	0.593	0.633	0.654	0.667	0.683	*0.719*
40	*0.917*	*0.734*	*0.726*	0.727	0.750	0.766	0.778	0.784	*0.820*
50	*0.945*	*0.837*	*0.831*	0.834	0.853	0.869	0.881	0.886	*0.912*
60	*0.976*	*0.906*	*0.907*	0.912	0.931	0.942	0.960	0.964	*0.974*
70	*0.981*	*0.929*	*0.954*	0.964	0.989	1.001	1.008	1.004	*1.011*
75	0.947	*0.938*	*0.961*	0.978	1.006	1.021	1.029	1.024	*1.033*
80	*0.992*	*0.955*	*0.959*	0.972	1.017	1.035	1.046	1.037	*1.043*
85	*1.007*	*0.973*	0.960	0.982	0.998	1.030	1.041	1.036	*1.043*
$\phi_{an}(r)$	*1.130*	*0.880*	*0.859*	0.855	0.870	0.884	0.895	0.897	*0.918*

metric model, $\%\sigma_{Y|\text{geo}}$; and the type A statistical uncertainty, $\%\sigma_{Y|s}$ inherent to the Monte Carlo technique. Applying Eq. (15), one obtains

$$\%\sigma_Y = \sqrt{\%\sigma_{Y|\mu}^2 + \%\sigma_{Y|\text{geo}}^2 + \%\sigma_{Y|s}^2} = \sqrt{\left(\%\frac{\partial Y}{\partial \mu}\right)^2 \%\sigma_\mu^2 + \left(\%\frac{\partial Y}{\partial \text{geo}}\right)^2 \%\sigma_{Y|\text{geo}}^2 + \%\sigma_{Y|s}^2}, \tag{16}$$

where the relative uncertainty propagation factor is defined as

$$\%\frac{\partial Y}{\partial x} \equiv \frac{x}{Y}\frac{\partial Y}{\partial x}. \tag{17}$$

The variable x denotes either the cross-section value, μ, or geometric dimension, geo, of interest. The uncertainties estimated here are standard uncertainties, having a coverage factor of unity, approximating a 68% level of confidence.

1. Λ uncertainty

The influence of cross-section uncertainty was derived from the Monte Carlo data published by Hedtjarn *et al.*[42] This paper gives Monte Carlo estimates of Λ and $g(r)$ calculated for two different cross-section libraries, DLC-99 (circa 1983) and DLC-146 (1995). The photoelectric cross sections of the two libraries differ by about 2% between 1–40 keV, corresponding to a 1.1% change in μ for the mean photon energy emitted by ^{125}I. Using these data to numerically estimate the derivative in Eq. (17), one obtains $\%\partial\Lambda/\partial\mu = 0.68$. Assuming that $\%\sigma_\mu = 2\%$,[43] then uncertainty in Λ due only to cross-section uncertainty, $\%\sigma_{\Lambda|\mu}$, is 1.4%.

TABLE XI. $F(r,\theta)$ for NASI model MED3633.

Polar angle θ (degrees)	r [cm]					
	0.25	0.5	1	2	5	10
0	1.024	0.667	0.566	0.589	0.609	0.733
10	0.888	0.581	0.536	0.536	0.569	0.641
20	0.850	0.627	0.603	0.614	0.652	0.716
30	0.892	0.748	0.729	0.734	0.756	0.786
40	0.931	0.838	0.821	0.824	0.837	0.853
50	0.952	0.897	0.890	0.891	0.901	0.905
60	0.971	0.942	0.942	0.940	0.948	0.939
70	0.995	0.976	0.974	0.973	0.980	0.974
80	1.003	0.994	0.997	0.994	1.000	0.986
$\phi_{an}(r)$	1.257	0.962	0.903	0.895	0.898	0.917

TABLE XII. Generic uncertainty assessment for experimental measurements using TLDs, and Monte Carlo methods for radiation transport calculations. Type A and B uncertainties correspond to statistical and systematic uncertainties, respectively. All values provided are for 1 σ.

TLD uncertainties		
Component	Type A	Type B
Repetitive measurements	4.5%	
TLD dose calibration (including linac calibration)		2.0%
LiF energy correction		5.0%
Measurement medium correction factor		3.0%
Seed/TLD positioning		4.0%
Quadrature sum	4.5%	7.3%
Total uncertainty	8.6%	
ADCL S_K uncertainty	1.5%	
Total combined uncertainty in Λ	8.7%	

Monte Carlo uncertainties		
Component	$r=1$ cm	$r=5$ cm
Statistics	0.3%	1.0%
Photoionization[a]	1.5%	4.5%
Cross-sections (2.3%)		
Seed geometry	2.0%	2.0%
Source energy spectrum[a]	0.1%	0.3%
Quadrature sum	2.5%	5.0%

[a]On the transverse plane.

Estimation of geometric uncertainty, $\%\sigma_{\Lambda|G}$, is a complex and poorly understood undertaking. Each source design is characterized by numerous and unique geometric parameters, most of which have unknown and potentially correlated probability distributions. However, a few papers in the literature report parametric studies, in which the sensitivity of dosimetric parameters to specified sources of geometric variability is documented. For example, Williamson has shown that the distance between the two radioactive spherical pellets of the DraxImage ^{125}I source varies from 3.50 to 3.77 mm.[44] This leads to a source-orientation dependent variation of approximately 5% in calculated dose-rate constant. Rivard published a similar finding for the NASI model MED3631-A/M ^{125}I source.[45] If this phenomenon is modeled by a Type B rectangular distribution bounded by the minimum and maximum Λ values, the standard uncertainty is given by

$$\%\sigma_{\Lambda|\text{geo}}=100\frac{|\Lambda_{\max}-\Lambda_{\min}|}{2\bar{\Lambda}\sqrt{3}}. \tag{18}$$

For the DraxImage source, Eq. (18) yields a $\%\sigma_{\Lambda|\text{geo}}=1.4\%$. For the Theragenics Corporation Model 200 seed, Williamson has shown that Λ is relatively insensitive to Pd metal layer thickness or end weld configuration.[46] Thus 2% seems to be a reasonable and conservative estimate of $\%\sigma_{\Lambda|\text{geo}}$.

The reported statistical precision of Monte Carlo Λ estimates ranges from 0.5% for Williamson's recent studies to 3% for Rivard's MED3631-A/M study.[44,45] Thus for a typical Williamson study, one obtains a $\%\sigma_\Lambda$ of 2.5%. Using the $\%\sigma_{\Lambda|s}$ reported by each investigator along with the standard $\%\sigma_{\Lambda|\text{geo}}$ and $\%\sigma_{\Lambda|\mu}$ values, discussed above, $\%\sigma_\Lambda$ varies from 2.5% to 3.7% for the eight seeds described in this report. Thus, assuming a standard or generic $\%\sigma_\Lambda$ of 3% for all Monte Carlo studies seems reasonable.

2. $_{\text{CON}}\Lambda$ uncertainty

This report defines the consensus dose-rate constant as

$$_{\text{CON}}\Lambda=\alpha\cdot{}_{\text{EXP}}\Lambda+(1-\alpha)\cdot{}_{\text{MC}}\Lambda,$$

where $\alpha=0.5$. Applying the LPU law from Eq. (15), obtains

$$\%\sigma^2_{{}_{\text{CON}}\Lambda}=\alpha^2\left(\frac{{}_{\text{EXP}}\Lambda}{{}_{\text{CON}}\Lambda}\right)^2\%\sigma^2_{{}_{\text{EXP}}\Lambda}+(1-\alpha)^2\left(\frac{{}_{\text{MC}}\Lambda}{{}_{\text{CON}}\Lambda}\right)^2\%\sigma^2_{{}_{\text{MC}}\Lambda}+(\%\sigma_B)^2. \tag{19}$$

$\%\sigma_B$ is an additional component of uncertainty in $_{\text{CON}}\Lambda$ due to the possible bias in the average of the results of experimental and Monte Carlo methods, and is modeled by a Type B rectangular distribution, bounded by $_{\text{EXP}}\Lambda$ and $_{\text{MC}}\Lambda$.[47] The bias B is assumed to be equal to zero, with standard uncertainty given by $\%\sigma_B=100|{}_{\text{EXP}}\Lambda-{}_{\text{MC}}\Lambda|/(2\sqrt{3}{}_{\text{CON}}\Lambda)$. For the various seed models presented in this protocol, $\%\sigma_B$ varies from 0.4% to 1.5%, depending on the magnitude of the discrepancy between Monte Carlo and TLD results. Assuming $\%\sigma_{{}_{\text{EXP}}\Lambda}=8.7\%$ along with model-specific $\%\sigma_{{}_{\text{MC}}\Lambda}$ and $\%\sigma_B$ values, $\%\sigma_{{}_{\text{CON}}\Lambda}$ varies from 4.6% to 5.0%. Thus for the purposes of practical uncertainty assessment, a model independent $\%\sigma_{{}_{\text{CON}}\Lambda}$ value of 4.8% is recommended.

As common in the field of metrology, future changes and improvements to the NIST WAFAC air-kerma strength measurement system and other calibration standards are expected, and may somewhat impact dose rate constant values. For example, the international metrology system has recently revised the ^{60}Co air-kerma standard for teletherapy beams. Consequently, NIST has revised its ^{60}Co air-kerma standard effective July 1, 2003 by about 1% due to new, Monte Carlo based wall corrections (k_{wall}) for graphite-wall ionization chambers. Changes in the NIST ^{60}Co air-kerma strength standard, which is the basis for AAPM TG-51 teletherapy beam calibrations, will only affect (i) detectors calibrated using either ^{60}Co beams directly, or (ii) detectors calibrated using high-energy photon beams (e.g., 6 MV) calibrated with ionization chambers which were themselves calibrated using the ^{60}Co standard. As long as these changes are small in comparison to the aforementioned value of 8.7%, the clinical medical physicist need not be immediately concerned.

3. $g(r)$ uncertainty

For the sources considered in this report, except for the NASI model MED3631-A/M ^{125}I source, the Monte Carlo-derived values, ${}_{MC}g(r)$, were adopted as the consensus dataset for radial dose function, ${}_{CON}g(r)$. For this one seed, the ${}_{CON}g(r)$ values were based on diode measurements by Li *et al.*[48] Therefore, an uncertainty analysis of both ${}_{MC}g(r)$ and ${}_{EXP}g(r)$ are presented separately.

Since ${}_{MC}g(r)$ is a relative quantity that is not combined with experimental results which are used only for 0 0im6m(for)-288d* [iteisasumned tateexperimentaldatd notcotrib-r

effects of anisotropy; the analysis presented herein is neither complete nor rigorous: the AAPM supports further research in the area of brachytherapy dose-calculation uncertainties.

V. RECOMMENDED METHODOLOGY TO OBTAIN BRACHYTHERAPY DOSIMETRY PARAMETERS

In this section, the AAPM recommends a list of methodological details that should be described in brachytherapy dosimetry publications based upon either experimental or theoretical methods, along with more prescriptive guidelines on performing such studies. The list of key details documented in this report for each study is reviewed later. To better appreciate results from a particular dosimetric measurement and its uncertainties, the reader is referred to a listing of parameters needed to assess data for TLD measurements.[50] Unfortunately, this level of description was not realized in many of the papers cited. When key data or methodological details were missing from a published paper, the author was contacted and asked to provide the missing information.

A. General recommendations

Since publication of TG-43,[1] the LIBD has published guidelines on dosimetric prerequisites for low-energy photon-emitting interstitial brachytherapy sources.[9] The aim of those recommendations was to assure that multiple dosimetry studies, each subjected to the rigors of the peer-review process, were available for each source model. However, that publication gave few technical guidelines to investigators publishing reference-quality dose-rate distributions derived from measurements or radiation transport calculations. Based on the LIBD experience of analyzing dosimetry datasets,[35] more detailed recommendations on dosimetry methodology and data analysis are presented in this section. These recommendations are intended to define minimum requirements for future source dosimetry studies so that the accuracy and consistency of the consensus datasets may be improved.

B. Preparation of dosimetry parameters

Dosimetric parameters should be tabulated for both 1D and 2D dose-calculation models. This will require the investigator to calculate the geometry function and the radial dose function using both point-source (1D) and line-source (2D) geometry functions (see Sec. III A 3). Consequently, the investigator should always specify the active length used for the 2D line-source geometry function. As previously stated in Sec. III B, Eq. (11) is the recommended formalism for the 1D approximation.

Specification of dosimetry parameters at a few distances or angles will not allow a sufficiently complete or accurate dose reconstruction of the 2D dose distribution adequate for clinical implementation. In many instances, the underlying dose distribution will have high gradients. Inadequate spatial resolution may result in inaccurate interpolation by brachytherapy treatment planning systems, unnecessarily giving rise to dose-delivery errors. Therefore, it is necessary to recommend minimum spatial resolutions and ranges for which these parameters should be specified.

1. Air-kerma strength

For experimental measurement of absolute dose rates to water, at least one source should have direct traceability of S_K to the 1999 NIST WAFAC calibration standard. Other sources used in the experiment should have a precisely transferred air-kerma strength using high-precision transfer devices such as well-characterized well-ionization chambers and secondary standards maintained by the investigator as well as the manufacturer's laboratories. The investigator using experimental techniques should state the NIST S_K calibration uncertainty in the evaluation of Λ. Use of another source, *even the same model*, to cross-calibrate dosimeters for the determination of Λ is *highly discouraged* since uncertainties propagate and hidden errors may exist.

2. Dose-rate constant

The experimental investigator should rigorously control and try to minimize all detector response artifacts such as dose-rate dependence, dose response nonlinearity, energy dependence, volumetric averaging, temporal stability of readings and calibration coefficients, and accuracy of detector positioning both in the source measurement setup and the detector calibration setup. These issues should be discussed in the measurement methodology section of the published paper, and a rigorous uncertainty analysis should also be provided.

Experimentally, Λ is evaluated by taking the ratio of the absolute dose rate, $\dot{D}(r_0,\theta_0)$ (the only absolute dose rate required to define TG-43 dosimetry parameters) and the measured air-kerma strength of the source, decayed to the time of dose-rate measurement. Typically 8–10 sources are used, with at least one source having direct traceability to a NIST calibration. At least 15 measurements of $\dot{D}(r_0,\theta_0)$ are generally performed. For example, multiple measurements of $\dot{D}(r_0,\theta_0)$ around a ist1n-

The parameter $\dot{d}(r_0, \theta_0)$ is the dose rate per history estimated using Monte Carlo methods at the reference position, and s_K is the air-kerma strength per history estimated using Monte Carlo methods. Note the lower-case notation used to differentiate the normalized parameter, e.g., dose rate per history ($\mathrm{cGy\,h^{-1}\,history^{-1}}$) as compared to absolute dose rate ($\mathrm{cGy\,h^{-1}}$). Although Monte Carlo studies are potentially free from experimental artifacts such as positioning uncertainties, energy response corrections, and signal-to-noise ra-

TABLE XIV. Composition (percent mass) of air as a function of relative humidity at a pressure of 101.325 kPa.

Relative humidity (%)	Hydrogen	Carbon	Nitrogen	Oxygen	Argon
0	0.0000	0.0124	75.5268	23.1781	1.2827
10	0.0181	0.0124	75.4048	23.2841	1.2806
40	0.0732	0.0123	75.0325	23.6077	1.2743
60	0.1101	0.0123	74.7837	23.8238	1.2701
100	0.1842	0.0122	74.2835	24.2585	1.2616

5. 1D anisotropy function

To derive 1D anisotropy function data, a solid-angle weighted-average of the relative dose rates, uncorrected by the geometry function, should be performed over all angles. When examining small radii where $\theta = 0°$ or 180° would place the calculation point within the source, the weighting should exclude the capsule/source volume and include only the volume outside the encapsulation. This is easily calculated for radii, r, less than half the capsule length where $r \sin\theta > r_{cap}$, where r_{cap} is the outer radius of the capsule.

C. Reference data and conditions for brachytherapy dosimetry

1. Radionuclide data

Since publication of the 1995 TG-43 protocol, the half-lives, abundances and energies of photons emitted by unfiltered ^{125}I and ^{103}Pd sources have been re-evaluated by NIST.[52–55] The currently recommended values are presented in Table XIII. These values should be used to interpret future experimental measurements and as source spectra in Monte Carlo calculations. The recommended ^{125}I half-life is unchanged from the original TG-43 protocol. Differences between the recommended ^{103}Pd half-life and that reported in TG-43 yield differences in the decay corrections exceeding 1% only for decay times >200 days. Of note is that the ^{125}I spectrum should now be described in terms of five different photon energies (previously three) with a 5% increase in the number of photons per decay (previously 1.40). The ^{103}Pd emission spectrum should now be described in terms of eight discrete photon emissions (previously two) with a 4% decrease in the number of photons per decay (previously 0.8). Although the relative number of high-energy photons emitted by ^{103}Pd is low, their contribution to dose at distances beyond 10 cm can be clinically relevant and should also be considered for shielding calculations and exposure-control procedures.[56]

2. Reference media

Water continues to be the recommended medium for reference dosimetry of interstitial brachytherapy sources. For dosimetry calculations and measurements, it may be necessary to know the composition of various forms of water and air. Pure, degassed water is composed of two parts hydrogen atoms and one part oxygen atoms, with a mass density of 0.998 g cm^{-3} at 22 °C. Reference conditions for dry air are taken as 22 °C and 101.325 kPa (760 mm Hg) with a mass density of 0.001 196 g cm^{-3}. Since the composition of air may change as a function of relative humidity, Table XIV is provided to account for this effect.[57,58] The proportion by weight of water in air of 100% relative humidity varies only between 1% and 2%, for temperatures between 16 °C and 26 °C and pressures between 735 mm Hg and 780 mm Hg. The change in mass density of saturated air is no more than a 1% reduction with respect to that for dry air, over this range of temperatures and pressures. Thus, the mass density will be set at 0.001 20 g cm^{-3} for both dry and moist air. For Monte Carlo calculations, the recommended relative humidity is 40%, which corresponds to the relative humidity in an air-conditioned environment where measurements should be carried out.

D. Methodological recommendations for experimental dosimetry

Compared to Monte Carlo theorists who may idealize reality by a theoretic construct, the experimental investigator should address the variability that represents the clinical environment. The experimental study should investigate a reasonably large sample of sources received from multiple shipments at different stages of the production stream from the manufacturer.

1. Detector choice

LiF TLD remains the method of choice for the experimental determination of TG-43 dosimetry parameters for low-energy photon-emitting brachytherapy sources.[59–63] While a variety of other experimental dosimeters such as diodes, diamond detectors, miniature ionization chambers, plastic scintillators, liquid ionization chambers, polymer gels, radiographic and radiochromic film, and chemical dosimeters have been used for brachytherapy dosimetry,[48,49,64–80] their validity for obtaining brachytherapy dosimetry parameters has not yet been convincingly demonstrated for absolute dose-rate measurements near low-energy photon-emitting brachytherapy sources. For dosimetry parameters based on relative measurements, some of these other dosimeters have been successfully used. Diode detectors, in particular, are well established for relative measurements.[65,68,70] For ^{125}I, Li *et al.* has shown that the relative energy-response correction, although large, is independent of the point of measurement.[49] However, validity of the results of absolute and relative dosimetry parameters using these experimental dosimeters (other than LiF TLDs and diodes) remains to be demonstrated through comparison of results with established Monte

Carlo and experimental techniques using well-characterized ^{125}I or ^{103}Pd sources (such as those contained in this protocol). Multiple publications of results in peer-review journals by independent investigators (see the *second meaning* of ''independent studies'' in Sec. V F) are desirable to demonstrate independence and consistency. Therefore, use of these experimental dosimeters is an area of future research of significant scientific value. For measuring brachytherapy dosimetry parameters, detectors should have the following properties:

(a) Detectors should have a relatively small active volume such that effects of averaging of high-gradient dose fields over this volume are negligible or are accurately accounted for by correction coefficients.
(b) A well-characterized energy-response function such that differences between the calibration energy and experimentally measured energy are either negligible or may be quantitatively accounted for.
(c) Sufficient precision and reproducibility to permit dose-rate estimation with 1σ statistical (Type A) uncertainties $\leqslant 5\%$, and 1σ systematic uncertainties $<7\%$. For example, TLD statistical uncertainties may be improved through repeated measurement at a given location, and systematic uncertainties may be improved through measuring chip-specific calibration coefficients. Typical statistical and systematic uncertainties for $1\times1\times1$ mm^3 TLD-100 chips are 4% and 7%, respectively, with total combined uncertainties of 7–9 %.[81] Therefore, $1\times1\times1$ mm^3 TLD-100 chips are considered a valid detector to perform the aforementioned absolute and relative measurements.

Because none of the experimental dosimeters satisfy the above prerequisites for absolute dose measurement, LiF thermoluminescent dosimetry is currently the method of choice for experimental determination of the dose-rate constant and is the most extensively (but not only) validated methodology for relative dose measurement. Several important issues in TLD dosimetry are discussed in more detail in the following section.

2. Medium and energy response characterization

It is necessary that the measurement medium should also be well characterized.[82] While epoxy-based substitutes for water, such as Solid Water™ by Gammex-RMI or Virtual Water™ by MED-TEC Inc., have liquid–water conversion coefficients that differ from unity by less than 5% for high-energy teletherapy beams, coefficients range from within 5% to 15% from unity for low-energy photon-emitting sources. Recently, the measured calcium concentration of Solid Water™ was found to have deviated from the vendor's specification by as much as 30%.[59] Therefore, when Solid Water™ is used in experimental dosimetry, the atomic composition of the material used should be measured and correction coefficients based on the measured composition of Solid Water™ should be used. Although Solid Water™ is the most widely used material for TG-43 reference dosimetry, it has several shortcomings. In addition to concerns over the constancy of its composition, Solid Water™ and similar water substitutes require solid-to-liquid water conversion corrections ranging from within 5% to 15% from unity in the 1–5 cm range. Alternative materials need to be researched by future investigators. Because some of the low-Z media such as polystyrene, polymethylmethacrylate, or plastic water (model PW2030 by Computerized Imaging Reference Systems, Inc.) generally have more uniform and better-characterized compositions, these media may be possible candidates for future low-energy photon-emitting brachytherapy dosimetry studies. However, values for their plastic-to-water conversion coefficients, which are expected to be larger than corresponding Solid Water™ corrections, need to be accurately determined for dosimetrically well-characterized source models, such as those covered in this protocol, and validated by independent investigators in peer-reviewed publications.

The relative energy response correction, $E(r)$, is the largest single source of Type B (systematic) uncertainty for TLD and other secondary dosimeters used in brachytherapy dosimetry. It is defined as the ratio of TLD response per unit dose in water medium at position r in the brachytherapy source geometry, to its response per unit dose in the calibration geometry, usually a calibrated ^{60}Co or 6 MV x-ray beam.[83] In general, $E(r)$ depends on source-to-detector distance,[83] r, and may include corrections for volume averaging (influence of dose gradients in the TLD volume), detector self-absorption, medium displacement, and conversion from the measurement medium to liquid water. Most investigators treat $E(r)$ as a distance-independent constant, although when it includes volume-averaging and solid-to-liquid water corrections, as is often the case for Monte Carlo estimates, $E(r)$ varies significantly with distance.[59] This correction can be evaluated by irradiating TLD detectors to a known dose in free space in a calibration low-energy x-ray beam having a spectrum that matches the brachytherapy spectrum of interest. For TLD-100 and liquid-water measurement medium, values ranging from 1.39 to 1.44 for ^{125}I, relative to 4 MV x rays or ^{60}Co rays, have been reported.[84–86] For ^{125}I, Meigooni *et al.* and Reft have shown that $E(r)$ values inferred from in-air measurements depend on TLD size.[82,86] Since free-air measurements relate TLD reading to dose in a void left by removing the chip, a replacement correction (2%–5%), is needed to correct for the phantom material displaced by the detector. However, precise measurement of $E(r)$ is difficult because (i) photons from the low-energy tail of the Bremsstrahlung spectrum bias the measurements to an unknown extent, (ii) the limited precision of TLD readout, and (iii) the relatively large uncertainty of ion chamber dosimetry in this energy range. Recent authors have assigned an uncertainty of 5% to $E(r)$.[86,87] An alternative to the experimental approach is to calculate $E(r)$ directly by Monte Carlo simulation.[59,83] Although volume-averaging, displacement and detector self-attenuation corrections can be easily included, the method assumes that TLD response is proportional to energy imparted to the detector (intrinsic linearity), an assumption which has been questioned for some TLD phosphors and annealing and glow-curve analysis techniques.[62] For the widely used TLD-100

chips using Cameron annealing and readout techniques, the evidence for intrinsic linearity is controversial. Das *et al.* compared the Monte Carlo and the experimental free-air x-ray beam approaches. Their measured relative responses (1.42–1.48) were in good agreement (relative to stated 4% experimental precision) with measurements reported by other investigators and with their own Monte Carlo calculations.[63] However, a recent paper by Davis *et al.* concludes the opposite, that the measured TLD-100 energy response correction is underestimated by Monte Carlo calculations by 10% to 5% in the 24 to 47 keV energy range.[88] Their measured $E(r)$ values, which have stated uncertainty of 0.6%, are about 10% larger than previously reported measurements,[63,84–86] having values ranging from 1.58 to 1.61 in the ^{103}Pd–^{125}I energy range.

In utilizing measured or Monte Carlo $E(r)$ estimates published by others, LIBD recommends that TLD experimentalists confirm that the associated measurement methodology matches their dosimetry technique with regard to TLD detector type and size, annealing and readout technique, and megavoltage beam calibration technique. The latter requires accounting for differences in calibration phantom material and dose-specification media used by the experimentalist and assumed by the selected $E(r)$ estimate. The experimentalist should confirm the appropriate volume averaging, displacement, and self-absorption corrections regardless of whether they are included in $E(r)$ or applied separately. Finally, further research is needed to resolve the discrepancy between published $E(r)$ values, to identify the appropriate role for transport calculations in TLD dosimetry, and to reduce the large uncertainty associated with relative energy-response corrections.

3. Specification of measurement methodology

The experimental investigator should describe the following important features of the measurement materials and methods to permit assessment of the results:

(1) description of the external and internal source geometry,
(2) brachytherapy source irradiation geometry, orientation, and irradiation timeline,
(3) radiation detector calibration technique (including protocol from which the technique is derived) and energy response function, $E(r)$,
(4) radiation detector (dimensions, model No., and vendor) and readout system (e.g., electrometer unit model No. and settings, or TLD readout unit model No., vendor, time-temperature profiles, and annealing program),
(5) measurement phantom (composition, mass density, dimensions, model No., and vendor),
(6) phantom dimensions and use of backscatter (at least 5 cm backscatter is recommended for ^{125}I and ^{103}Pd dosimetry measurements),
(7) estimation of the impact of volume averaging on the results at all detector positions,
(8) number of repeated readings at each position, the number of different sources used, and the standard deviation of the repeated readings,
(9) NIST S_K value and uncertainty used for the measured source(s), and
(10) uncertainty analysis section assessing statistical and systematic uncertainties and their cumulative impact.

E. Methodological recommendations for Monte Carlo-based dosimetry

Monte Carlo codes used to model photon transport for brachytherapy dose calculation should be able to support detailed 3D modeling of source geometry and appropriate dose-estimation techniques. In addition, they should be based upon modern cross-section libraries and a sufficiently complete model of photon scattering, absorption, and secondary photon creation. Codes that have been widely used for interstitial brachytherapy dosimetry include EGS, MCNP, and Williamson's PTRAN code.[89–91] These codes have been widely benchmarked against experimental measurements or each other, so that their appropriate operating parameters and limitations can be considered to be well understood.[68] In general, the AAPM recommends Monte Carlo investigators utilize such well-benchmarked codes for brachytherapy dosimetry studies intended to produce reference-quality dose-rate distributions for clinical use. However, regardless of the transport code chosen and its pedigree, all investigators should assure themselves that they are able to reproduce previously published dose distributions for at least one widely used brachytherapy source model. This exercise should be repeated whenever new features of the code are explored, upon installing a new code version, or as part of orienting a new user. Other radiation transport codes, including Monte Carlo codes not previously used in brachytherapy dosimetry, should be more rigorously tested and documented in the peer-reviewed literature before proposing to use their results clinically. This is especially true for other types of transport equation solutions, including multigroup Monte Carlo, discrete ordinates methods,[92] and integral transport solutions that have been proposed for brachytherapy dosimetry.[93,94]

Due to the short range of the secondary electrons produced by interactions from photons emitted by the radionuclides covered in this protocol, electron transport is not required and collision kerma closely approximates absorbed dose. Since the investigator performing Monte Carlo analysis can control many features of the transport calculations, it is imperative that the salient details be described in publications presenting Monte Carlo-derived brachytherapy dosimetry data. For instance, the collisional physics model should be described. The standard model used by experienced Monte Carlo users includes incoherent scattering corrected for electron binding by means of the incoherent scattering factor, coherent scattering derived by applying the atomic form factor to the Thompson cross section, and explicit simulation of characteristic x-ray emission following photoelectric absorption in medium- and high-atomic number media. For sources containing Ag or Pd, it is imperative that, if characteristic x-ray production is not explicitly simulated, the primary source spectrum be appropriately augmented to include their presence.

1. Specification of Monte Carlo calculation methodology

A list of key features that should be specified by the investigator in the publication follows:

(1) radiation transport code name, version number, and major options if any,
(2) cross-section library name, version number, and customizations performed if any,
(3) radiation spectrum of the source (consider Table XIII in Sec. V C 1),
(4) manner in which dose-to-water and air-kerma strength are calculated: name of estimator or tally, whether or not transport was performed in air and how attenuation correction coefficients were applied, and how suppression of contaminant x-ray production for $\dot{k}_\delta(d)$ calculations was performed to be compliant with the NIST $S_{K,N99}$ standard,
(5) source geometry, phantom geometry, and sampling space within the phantom,
(6) composition and mass density of the materials used in the brachytherapy source,
(7) composition and mass density of the phantom media,
(8) physical distribution of the radioisotope within the source, and
(9) uncertainty analysis section assessing statistical and systematic uncertainties and their cumulative impact.

2. Good practice for Monte Carlo calculations

For calculating brachytherapy dosimetry parameters, the following requirements should be adhered to:

(1) Primary dosimetry calculations should be performed in a 30 cm diameter liquid water phantom, but calculations in Solid Water™ may also be performed to supplement experimental results, e.g., calculation of $E(r)$, performed in Solid Water™ or other solid water substitutes. Typical calculations will produce dosimetry results extending out to $r \sim 10$ cm, with at least 5 cm of backscatter material for ^{125}I and ^{103}Pd dosimetry calculations.
(2) Enough histories should be calculated to ensure that dosimetry results have a 1σ ($k=1$, 67% confidence index) $\leqslant 2\%$ at $r \leqslant 5$ cm, and that $\dot{k}_\delta(d)$ calculations for derivation of s_K, have $1\sigma \leqslant 1\%$ at the point of interest.
(3) Modern, post-1980 cross-section libraries should be used, preferably those equivalent to the current NIST XCOM database such as DLC-146 or EPDL97. Exclude or appropriately modify older cross-section libraries based on Storm and Israel data.[96,97] Note that EGS4, EGSnrc, and MCNP all currently require modification or replacement of their default photoionization cross sections to meet this requirement. Furthermore, moist air best-describes experimental conditions in comparison to dry air (see Sec. V C 2), and mass-energy absorption coefficients for moist air are recommended to minimize systematic uncertainties.
(4) Manufacturer-reported source dimensions and compositions of encapsulation and internal components should be verified through the use of physical measurements,[45] transmission radiography,[44] and autoradiography.[98] Just as the TLD experimentalist should measure an appropriate sample of sources, the Monte Carlo investigator should quantify the geometric variations in a sample of similar size.
(5) The impact of volume-averaging artifacts should be limited to $<1\%$ through the appropriate choice of estimators (tallies) and scoring voxels if used.
(6) Calculations of $d(r,\theta)$ to derive $F(r,\theta)$ should include high-resolution sampling in high-gradient regions such as near the source ends or in regions where internal source shielding causes abrupt changes in $d(r,\theta)$ and subsequently $F(r,\theta)$.
(7) $k(d)$ should be modeled as a function of polar angle for s_K simulation and Λ derivation. Williamson has shown that for some sources, detectors with large angular sampling volumes (such as the NIST WAFAC) will have a significantly different response than point-kerma detectors positioned on the transverse-plane (see Appendix B.2.2 for greater detail). When the radioactivity is dispersed within or on the surface of a high-density core with sharp corners and edges, it may be necessary to simulate, if only approximately, the WAFAC geometry (dimensions and composition) to permit investigators the opportunity to directly compare Monte Carlo calculations of Λ with NIST-based measurements of Λ.
(8) Point source modeling is unacceptable.[95]
(9) Mechanical mobility of the internal source structures, which has the potential to significantly affect the dose distribution, should be considered by the Monte Carlo investigator in developing both the geometric model of the source and the uncertainty budget.[44,45]

F. Publication of dosimetry results

Previous AAPM recommendations stated that dosimetry results should be published preceding clinical implementation.[9] However, the journal *Medical Physics* established a ''seed policy'' in 2001 that, in effect, limits printing of articles to Technical Notes unless they contain significant new science. In order to comply with this restriction imposed by the journal, the AAPM will accept technical notes with limited details as acceptable, provided the full details as listed above are available to the committee at the time of evaluation. This policy in no way prevents publication of the article in other journals, as other scientific journals of interest to medical physicists are appropriate venues for publication of these dosimetry parameters.

In a 1998 report,[9] the AAPM recommended that dosimetry results be published by independent investigators, but did not offer a strict definition of what this independence entails. The spirit of the initial recommendation was to prompt publication of multiple studies to assess all the TG-43 brachytherapy dosimetry parameters, e.g., Λ, $g(r)$, $F(r,\theta)$, and $\phi(r)$. Through determining the consensus datasets for the brachytherapy sources evaluated in this protocol, a rigorous definition of the ''Independence Policy'' was adopted. There

are *two* aspects of this policy, and both shall be met for full compliance.

> The *first meaning* of ''independent studies'' is that they are performed, written, and published by investigators who are affiliated with institutions independent of the source vendor and who have no major conflicts-of-interest with that vendor.
>
> The *second meaning* of ''independent studies'' is that they are scientifically independent of one another, i.e., they represent independent and distinct estimations of the same quantities. In the case of two measurement-based studies, this will usually mean that two different investigators have used their own methodologies for measuring Λ and sampling the relative dose distribution, as TLD dosimetry is highly technique and investigator dependent. In the case of an empirical study and a Monte Carlo study, if properly executed, they will yield scientifically independent estimates of the TG-43 parameters. Thus, so long as the two studies are successfully scrutinized by the peer-review process and satisfy the AAPM scientific requirements, the empirical and Monte Carlo investigator author lists can overlap or even be identical. It is permissible to publish the Monte Carlo and measured estimates in the same paper so long as the two datasets are independently tabulated. In this context, ''Not independent'' means that the one study is used to modify the outcomes and methods of the other to improve agreement between the two datasets in a manner that is not scientifically justified.

When possible, the authors should cite previous publications where the measurement system or techniques were first described, and illustrate only the key features. It does not benefit either the reader or the journal in question to continually restate the definition of TG-43 parameters or their formalism. Simply citing this protocol or the original TG-43 publication will suffice.

VI. CLINICAL IMPLEMENTATION

Dose distributions in and around clinical interstitial implants are calculated using computerized radiotherapy treatment planning (RTP) systems. For sources with radio-opaque markers, the 3D coordinates of the centers (or the two ends) of the markers in implanted sources are determined using multiple-view radiographs or CT scans. The dose-rate contributions from each source at the points of interest are calculated using a one-dimensional or two-dimensional dose-calculation algorithm. These contributions are then summed to determine the total dose rate. This procedure assumes that there are no source-to-source shielding effects, that all tissues in and around the implant are water equivalent, and that the scattering volume within the patient is equivalent to that used in the consensus datasets. The term equivalent in this context means at least 5 cm of water-equivalent material surrounds the point of calculation. Many RTP systems are available commercially and use a variety of methods to calculate clinical dose-rate distributions. Some of the RTP systems use the single-source dosimetry data in a tabular form as input, whereas others represent the data by means of a mathematical formula that requires input of certain coefficients. Some use the TG-43 dose-calculation formalism and others do not. In this section, procedures for clinical implementation of the updated dosimetry parameters recommended above are presented.

The medical physicist is reminded that before adopting the recommendations presented in this report, the physicist should implement the dose-calculation data and technique recommended by this report on his/her treatment planning system and quantitatively assess the influence of this action on dose delivery. This is best done by comparing the dose distribution for typical implants based on the revised dose-calculation procedure with those based upon the currently implemented algorithm for the same seed locations, source strengths, and dose-calculation grid. The potential impact of these dose-calculation modifications on dose delivery relative to the current dose-calculation technique should be discussed with the appropriate radiation oncologist before clinically implementing the recommendations of this report. Finally, the comparison of old and new dose-calculation algorithms for the same seed input data, and the resultant decisions that may impact clinical dose delivery, should be documented for future reference and for regulatory purposes.

A. Dose-calculation formalism

doc. impFul-51.2(imppari-ia)-353.2(imp-399.2(impde6catn-346.2(impeas)46.

algorithm and perform calculations using methods *not* based upon Eqs. (1), (10), or (11). In most cases, one can devise a method to force the algorithm to generate the single-source dose-rate distributions recommended here by using modified values for the dosimetry parameters required by the RTP system. This conversion should be performed with care. As with RTP systems based on the TG-43 dose calculation formalism, one should assure that the RTP system is generating correct single-source dose-rate data by creating a single-source treatment plan with the modified parameters before clinical use. Meigooni *et al.* have described an example of this approach.[99] The methods used to arrive at modified data, as well as records of the evaluation of the RTP system, should be documented carefully and retained for use following installation of upgrades and for inspection by regulatory authorities. Extreme caution should be exercised whenever parameters should be entered or displayed that have units that do not match the units on documentation printed by the RTP system or displayed on its monitor. Procedures should be developed and documented to describe exactly how the modified data and parameters are related to the non-TG-43 parameters assumed by the RTP system. These procedures should address both clinical treatment planning practices and chart-checking procedures. Ratios of the unconventional units to the conventional units should be supplied, to facilitate review of the planning method. Because this approach is prone to errors in implementation or interpretation, this method should be used as the last resort. The AAPM recommends using RTP systems that comply fully with the TG-43 formalism, whenever possible.

B. Acceptance testing and commissioning

Before a new RTP system or a new source model on an established RTP system is used for patient treatment planning, thorough acceptance testing and commissioning shall be carried out. The user should document the results of these tests both for later reference, and for compliance with applicable regulations. As a minimum, calculations of the dose-rate distribution shall be performed for a single source of each type to be used clinically. The recommendations of the AAPM (TG-40, TG-53, and TG-56) should be followed.[100–102]

The dose rates calculated by the RTP system from a single source should be compared with the dose-rate distribution derived from the tabulated parameters and equations pre-

graphic dose display function of the RTP system, rather than a definitive test of the underlying dose-calculation algorithm. Because comparisons should include both point dose-rate calculations and the placement of isodose lines, the user should also ensure that the RTP system and its graphical output devices cause isodose curves to appear in the correct locations relative to corresponding point calculations.

C. Source calibrations

For calibrating radioactive sources, the AAPM has previously recommended that users not rely on the manufacturer's calibrations, but instead confirm the accuracy of source strength certificates themselves by making independent measurements of source-strength that are secondarily traceable to the primary standard maintained at NIST.[100] For patient treatments, AAPM further recommended that all clinically used sources bear calibrations that are secondarily traceable to the primary standard. AAPM defines ''direct traceability,'' ''secondary traceability,'' and ''secondary traceability with statistical inference'' as follows:[102]

> ''*Direct traceability* is established when either a source or a transfer instrument (e.g., well chamber) is calibrated against a national standard at an ADCL or at NIST itself.''
>
> ''*Snt*
>
> *Sirst*

aished when wa-344(wource)]344(ws)-344(won)]344(wf)-244(wa-344(wgroup]344(wf)-244(wources)-344(wf)-TJ T [(swica)]261*

toaceability,''

GLOSSARY OF SYMBOLS AND TERMS

AAPM — American Association of Physicists in Medicine

ADCL — AAPM-Accredited Dosimetry Calibration Laboratory

β — Angle subtended by $P(r,\theta)$ and the two ends of the active length. As used in the line source approximation, β has units of radians.

COMS — Collaborative Ocular Melanoma Study of episcleral eye plaque therapy versus enucleation trial.

d — Distance to the point of measurement from the source center in its transverse plane. Typically measured *in-air* or *in-vacuo*. Units of cm.

$\dot{d}(r_0,\theta_0)$ — The dose rate per history estimated using Monte Carlo methods at the reference position.

$\dot{D}(r,\theta)$ — Dose rate in water at $P(r,\theta)$. The dose rate is generally specified with units $\mathrm{cGy\,h^{-1}}$ and the reference dose rate, $\dot{D}(r_0,\theta_0)$, is specified at $P(r_0,\theta_0)$ with units of $\mathrm{cGy\,h^{-1}}$.

δ — Energy cutoff parameter used for air-kerma rate evaluation, which is 5 keV for this protocol.

FAC — Ritz parallel-plate free-air chamber developed by Loftus of NIST.

$F(r,\theta)$ — 2D anisotropy function describing the ratio of dose rate at radius r and angle θ around the source, relative to the dose rate at $r_0=1\,\mathrm{cm}$ and $\theta_0=90°$ when removing geometry function effects. Dimensionless units.

$G_X(r,\theta)$ — Geometry function approximating the influence of the radionuclide physical distribution on the dose distribution. $G_X(r,\theta)$ may be calculated by Monte Carlo simulation or by the following:

$G_P(r,\theta)=r^{-2}$ point-source approximation,

$$G_L(r,\theta)=\begin{cases}\dfrac{\beta}{Lr\sin\theta} & \text{if } \theta\neq 0°\\ (r^2-L^2/4)^{-1} & \text{if } \theta=0°\end{cases}$$

line-source approximation,

with units of $\mathrm{cm^{-2}}$.

$g(r)$ — Radial dose function describing the dose rate at distance r from the source relative to the dose rate at $r_0=1\,\mathrm{cm}$. Dimensionless units.

$g_L(r)$ — Radial dose function, determined under the assumption that the source can be represented as a line segment. Dimensionless units.

$g_P(r)$ — Radial dose function, determined under the assumption that the source can be represented as a point. Dimensionless units.

${}_{\mathrm{CON}}g(r)$ — Radial dose function derived from consensus dataset. Dimensionless units.

$\dot{k}_\delta(d)$ — Air-kerma rate per history *in vacuo* estimated using Monte Carlo methods, due to photons of energy greater than δ.

$\dot{K}_\delta(d)$ — Air-kerma rate *in vacuo* due to photons of energy greater than δ, with units of $\mathrm{cGy\,h^{-1}}$.

Λ — Dose-rate constant in water, with units of $\mu\mathrm{Gy\,h^{-1}\,U^{-1}}$. Λ is defined as the dose rate at $P(r_0,\theta_0)$ per unit S_K.

$\Lambda_{nnD,PqqS}$ — Notation identifying the dose-rate measurements or calculations used to determine $\dot{D}(r_0,\theta_0)$ and the calibration standard to which this dose rate is normalized. For example, $\Lambda_{97D,N99S}$ indicates a dose-rate constant determined from dosimetry measurements made in 1997 and having an S_K traceable to the 1999 NIST standard.

${}_{\mathrm{CON}}\Lambda$ — Notation indicating that the reported value of Λ is the consensus value determined by the AAPM from published data, with units of $\mathrm{cGy\,h^{-1}\,U^{-1}}$.

${}_{\mathrm{EXP}}\Lambda$ — Notation indicating that the reported value of Λ was determined by experimental measurement.

${}_{\mathrm{MC}}\Lambda$ — Notation indicating that the reported value of Λ was determined using Monte Carlo calculations.

L — Active length of the source (length of the radioactive portion of the source) with units of cm.

L_{eff} — Effective active length of the source, with units cm.

LIBD — Low-energy Interstitial Brachytherapy Dosimetry subcommittee of the AAPM Radiation Therapy Committee

NIST — National Institute of Standards and Technology

$P(r,\theta)$ — Point-of-interest, positioned at distance r and angle θ from the geometric center of the radionuclide distribution.

$\phi_{\mathrm{an}}(r)$ — The one-dimensional anisotropy function. At any radial distance r, $\phi_{\mathrm{an}}(r)$ is the ratio of dose rate averaged over 4π steradian integrated solid-angle to the dose rate at the same distance r on the transverse plane. Dimensionless units.

RTP — Radiotherapy planning system. In the context of this protocol, a treatment planning system that can perform dose calculations for brachytherapy implants.

r — The distance from the source center to $P(r,\theta)$, with units of cm.

r_0 — The reference distance, which is 1 cm for this protocol

s_K	The air-kerma strength per history estimated using Monte Carlo methods.
S_K	Air-kerma strength: the product of the air-kerma rate $\dot{K}_\delta(d)$ and the square of the distance d to the point of specification from the center of the source in its transverse plane. S_K is expressed in units of $\mu\text{Gy m}^2\,\text{h}^{-1}$, a unit also identified by U.
$S_{K,N85}$	The 1985 NIST FAC air-kerma standard.
$S_{K,N99}$	

the Loftus standard. Corrections for the new standard were made as were corrections for the Solid Water™ phantom to liquid water. The 6711 average ${}_{\mathrm{EXP}}\Lambda$ is 0.980 cGy h^{-1} U^{-1} and ${}_{\mathrm{MC}}\Lambda = 0.950$ cGy h^{-1} U^{-1} agree within 3%.[46,108] Because the LIBD is convinced the 6711 sharp edges phenomenon deserves further study, ${}_{\mathrm{MC}}\Lambda$ is the average of Williamson's air-kerma point detector and full WAFAC geometry simulations.

Similar methodology and results for the 6702 result in the average of the experimental values from the candidate datasets of Nath *et al.*, Chiu-Tsao *et al.*, and Weaver *et al.* being ${}_{\mathrm{EXP}}\Lambda = 1.0557$ cGy h^{-1} U^{-1}.[75–77] The average of the Monte Carlo values from the candidate datasets of Williamson[46,108] and Hedtjarn *et al.*[42] is ${}_{\mathrm{MC}}\Lambda = 1.0165$ cGy h^{-1} U^{-1}. Therefore the average of these values, ${}_{\mathrm{CON}}\Lambda$, is that presented in Table I.

1.2. 6702 and 6711 $g(r)$

For the model 6702 and the 6711 sources, the measured and Monte Carlo values for $r>1$ cm agree within the experimental uncertainties. The agreement is within 5% for the 6702 source and within 7% for the 6711 source. Table II shows ${}_{\mathrm{CON}}g(r)$ for both models (6702 and 6711), and for line- and point-source approximations. The references for the consensus datasets are provided.

For the 6702 source, measured results and Monte Carlo calculations for $r \geqslant 1$ cm agree to within 5% for $1<r<4$ cm and within 10% for distances greater than 4 cm. The Monte Carlo results of Hedtjarn *et al.*,[42] Williamson,[37] and Mainegra *et al.*[108] agree well with one another within the combined uncertainties. Monte Carlo results of Hedtjarn *et al.* are used since they are the most complete and are most consistent with other data for the model 6702 source.

Published data for the 6711 source indicate agreement between the experimentally measured values and the Monte Carlo calculations for distances greater than or equal to 1.0 cm. Experimental results agree to within 7% for $1<r<8$ cm. Monte Carlo results of Williamson and Mainegra *et al.* agree to within 3%.[37,110] The Monte Carlo values agree with experimental values to within 5%. Therefore, for 6711 $g(r)$, values from Williamson are used since the calculations cover a wider range, including $r<1$ cm.[37]

1.3. 6702 and 6711 $F(r,\theta)$

Experimental and Monte Carlo results agree within 5% at larger angles for both source models. Tables IV and V present the model 6702 and 6711 $F(r,\theta)$ data, respectively. The measured anisotropy functions $F(r,\theta)$ for the 6702 source from Nath *et al.*,[103] Furhang and Anderson,[105] Schell *et al.*,[65] and Chiu-Tsao *et al.*,[66] were compared with the Monte Carlo calculations of Weaver[95] and Capote *et al.*[111] In place of a realistic source geometry model used by other Monte Carlo investigators, Weaver used a simple line-source model for $F(r,\theta)$, in conjunction with a photon fluence anisotropy function measured in air at 100 cm for randomly selecting primary photon trajectories. Other than Furhang and Anderson, all datasets agree fairly well. The 2D anisotropy functions determined by Nath *et al.* and Capote *et al.* appear quite ''noisy'' and were therefore excluded from further analysis. The best remaining dataset is by Weaver. These data are the most uniform and complete, and are recommended as ${}_{\mathrm{CON}}F(r,\theta)$ in (Table IV).

The anisotropy functions $F(r,\theta)$ for the 6711 source from Sloboda and Menon,[104] Furhang and Anderson, and Chiu-Tsao *et al.*, were compared with Monte Carlo calculations by Weaver.[95] Other than Sloboda and Menon, and Furhang and Anderson, there is good agreement. The $1<r<5$ cm results for all angles are within 10%, with the exception of $F(1,0°)$. The most uniform and complete dataset seems to be Weaver, and therefore results by Weaver are recommended as the ${}_{\mathrm{CON}}F(r,\theta)$ in Table V for the model 6711 source.

2. Best medical model 2301 ^{125}I source

In 1992, a double walled encapsulated source of radioactive ^{125}I on a tungsten substrate was developed for interstitial brachytherapy (Best Medical International, Springfield, VA. model 2300) as described by Rustgi.[113] A sketch of this source is shown in Fig. 2(c). The double walled encapsulation design was intended to provide thinner walls at the ends of the source so that the corresponding angular distributions are more isotropic. In contrast to the model 6711 source, which uses a silver substrate that also serves as the radiographic x-ray marker for source localization in the patient, the model 2300 uses a tungsten rod. ^{125}I is distributed within a low atomic number cylindrical annulus that surrounds the rod (much like the Bebig source). Because the tungsten K-shell binding energy exceeds the maximum energy emitted during ^{125}I decay, no characteristic K-shell x-rays are produced whereas L-shell x rays are readily absorbed in the encapsulation.

In 1993, Nath and Melillo reported the dosimetric characteristics of the model 2300 source.[114] Six years later in 1999, the manufacturer introduced a commercial product based on the earlier design, which has been designated as the model 2301 source. The model 2301 source has a physical length of 4.95 mm and outer diameter of 0.8 mm. The ^{125}I radionuclide was infused within the organic matrix that was coated on a tungsten rod with an active length of 3.95 mm and a diameter of 0.25 mm [Fig. 2(c)]. Also in 1999, NIST established a WAFAC calibration standard for the air-kerma strength of the model 2301 source.

Meigooni *et al.* measured the TG-43 dosimetric parameters for the model 2301 source and reported the values based upon the original WAFAC 1999 standard.[115] Because of the 1999 NIST WAFAC anomaly, which was discovered after the publication of Meigooni *et al.*, the air-kerma strength was revised, the value determined as in Table I, and the TG-43 dosimetry parameters reported by Meigooni *et al.* were corrected to this new value. In 2002, Nath and Yue published independent determinations of TG-43 parameters of the model 2301 source based on TLD measurements.[116]

Finally, Sowards and Meigooni published a TG-43 dosimetry dataset obtained using Monte Carlo methods in both liquid water and Solid Water™.[117]

2.1. 2301 Λ

For comparison purposes, Sowards and Meigooni published a dose rate constant value of 0.98 ± 0.03 cGy h^{-1} U^{-1} in Solid Water™, and obtained $_{MC}\Lambda = 1.01 \pm 0.03$ cGy h^{-1} U^{-1} in liquid water.[117]

In a Solid Water™ phantom, Nath and Yue used LiF TLD detectors which were calibrated against a 6 MV x-ray beam.[116] A relative energy-response correction factor of 1.41 was used.[83] Nath's published Λ value was increased by 4.3%, based on ^{125}I Monte Carlo simulations, to correct for nonwater equivalence of the Solid Water™[37] measurement medium, yielding $\Lambda = 1.02 \pm 0.07$ cGy h^{-1} U^{-1}. Meigooni *et al.* have also measured $_{EXP}\Lambda$ using LiF TLDs in a Solid Water™ phantom using a 6 MV x-ray beam for calibration and a relative energy response correction factor of 1.40. The authors applied 1.05 as the correction factor to account for the Solid Water™ measurement medium. After applying the 1999 WAFAC anomaly correction to the published value, a value of $\Lambda = 1.01 \pm 0.08$ cGy h^{-1} U^{-1} was obtained based on the authors' uncertainty analysis.[115] A further correction was reported in a private communication that resulted in a final value of $\Lambda = 1.03$ cGy h^{-1} U^{-1} for the Meigooni group,[86] as described in detail within the publication by Nath and Yue.[116]

In this protocol, the final measured values of the candidate datasets of Nath and Yue and of Meigooni *et al.* were averaged to obtain a mean value of $_{EXP}\Lambda = 1.025$ cGy h^{-1} U^{-1}. This mean measured value was averaged with $_{MC}\Lambda = 1.01$ cGy h^{-1} U^{-1} yielding $_{CON}\Lambda = 1.018$ cGy h^{-1} U^{-1}.

2.2. 2301 $g(r)$

The measured radial dose function of Meigooni *et al.*[115] for the Best model 2301 source is slightly more-penetrating than that of model 6711 ^{125}I source, and slightly less penetrating than that of the model 6702 ^{125}I source at distances beyond 2 cm. Monte Carlo results from Sowards and Meigooni were chosen as the $_{CON}g(r)$; these values are presented in Table II.

2.3. 2301 $F(r,\theta)$

The anisotropy function of the Best ^{125}I source (model 2301) was measured at 2, 4, and 6 cm, and at different θ angles by Nath and Yue and at 2, 5, and 7 cm by Meigooni *et al.* Monte Carlo calculations at distances of 1, 2, 3, 4, 5, 6, and 7 cm were reported by Sowards and Meigooni. A comparison of the measured and calculated values indicates good agreement between the different datasets. Following the consensus procedure, $_{CON}F(r)$ was chosen based on results reported by Sowards and Meigooni with the exception of 6 cm data which exhibited larger statistical noise. Therefore, results from Sowards and Meigooni were used for $_{CON}F(r,\theta)$, and are presented in Table VI.

3. North American Scientific Inc. model MED3631-A/M ^{125}I source

The North American Scientific Inc. (NASI) model MED3631-A/M source[45,48,118,119] was introduced to the market in October 1998 following a brief appearance by the model MED3631-A/S source.[120–122] The capsule is made of titanium, with a 0.81 mm outer diameter and 0.05 mm wall thickness, and a nominal length of 4.5 mm with spherical end welds of thickness 0.05 to 0.15 mm. Inside the MED3631-A/M are four polystyrene ion exchange resin beads, within which ^{125}I is uniformly distributed. The four beads are separated into two sets by two gold-copper radiopaque markers. Both the beads and markers have a nominal diameter of 0.5 mm, and are free to move about within the capsule interior [Fig. 2(d)].

The only complete (2D) experimental characterization of brachytherapy dosimetry parameters was performed by Wallace and Fan.[120] They irradiated TLD-100 rods in tissue- and water-equivalent plastic phantoms. Detectors were calibrated using a ^{60}Co teletherapy beam with tissue-equivalent phantom corrections, $C_p(r)$, of $C_p(r=0.5\text{ cm}) = 0.778$ and $C_p(r=7\text{ cm}) = 1.053$. Measurements were performed in 1998, so corrections for the 1999 WAFAC anomaly were not necessary since the 2000 NIST WAFAC measurements differed by $<1\%$ compared to the 1998 calibration. Table I shows the value used now based on a 2001 calibration. Because the $G(r,\theta)$ used by all investigators was based on a four point source model, all $g(r)$ and $F(r,\theta)$ datasets were converted using an active length of 4.2 mm to adhere to the 2D formalism of this protocol.

Rivard published a complete, 2D TG-43 dosimetry dataset for the MED3631-A/M source using Monte Carlo methods developed from previous studies.[123–126] The effect of internal component motion on dose distributions external to the capsule was considered for the first time. The WAFAC was not simulated, and a 30 cm diameter liquid water spherical phantom encompassed the source. Radii ranged from 0.25 to 10 cm, and the angular range was 0° to 180° with 1° increments. Air-kerma strength was determined in a 6 meter diameter sphere of dry air by multiplying the total air-kerma strength, integrated over all photon energies, by 1.049 to account for photon transmission in air at 1 meter, and by 0.897 to account for Ti K-shell x rays. A corrected value was later published, recognizing that the $S_{K,N99}/S_{K,N85}$ factor measured by NIST does not accurately model the influence of Ti x rays in the geometry used for Monte Carlo calculations.[127] Statistical uncertainties ranged from 0.1% to 2% for $F(r,\theta)$ on the transverse plane to the source ends, respectively. Statistical uncertainties in $g(r)$ and Λ were typically $\leqslant 1\%$, and $\sim 3\%$, respectively.

3.1. MED3631-A/M Λ

Wallace and Fan reported $\Lambda = 1.056$ cGy h^{-1} U^{-1}, and Li *et al.* reported $\Lambda = 1.067$ cGy h^{-1} U^{-1}. This average yields $_{EXP}\Lambda = 1.0615$ cGy h^{-1} U^{-1}. Rivard calculated $\Lambda = 1.066$ cGy h^{-1} U^{-1}, but this value was later corrected to 1.011 cGy h^{-1} U^{-1} based on an inappropriate correction methodology.[127] Taking an equally weighted average of 1.0615 and 1.011, Table I shows $_{CON}\Lambda = 1.036$ cGy h^{-1} U^{-1}.

Li *et al.* performed measurements only on the transverse-plane in 1999.[48] Dosimetry measurements were made using

TLD-100 chips and a diode in a large water phantom. Irradiation in the water phantom was accomplished by taping the TLD chips onto the tip of the diode detector for 30 minutes. No phantom material correction was employed, but the TLD energy response function of Weaver *et al.* was used.[107] Calculation of Λ was based on the ratio of measured readings of MED3631-A/M and 6702 ^{125}I sources and using the 6702 source S_K value. Effectively, the TLD's were calibrated against the model 6702 source based upon the TG-43 Λ_{6702} value. Due to propagation of uncertainties from both 6711 and MED3631-A/M measurements into the final result, this protocol does not recommend the practice of cross calibration, and these values were omitted from the analysis. However, the Li *et al.* measurements were later used as ${}_{\mathrm{CON}}g(r)$.

3.2. MED3631-A/M $g(r)$

For determination of $g(r)$, Li *et al.* used the same geometry function as obtained above by Wallace and Fan. While the range of distances to the source covered by Rivard for determination of $g(r)$ was larger and closer than either Wallace and Fan or by Li *et al.*, the impact of outdated default photon cross-section libraries in MCNP has become recently apparent.[96] While by definition all datasets agree at r_0, differences between Rivard's $g(r)$ data and that of Li *et al.* and Wallace and Fan gradually increased—reaching 25% at 7 cm. Consequently, the difference between results obtained by Rivard and by Li *et al.* and by Wallace and Fan are not readily resolvable. Therefore, the measured data of Li *et al.* were chosen for the ${}_{\mathrm{CON}}g(r)$ data as they demonstrate more consistent behavior than that of Wallace and Fan. Agreement with the Wallace and Fan $g(r)$ data was within $\pm 5\%$ for $r < 6$ cm. Since the impact of differences as a function of distance is independent of normalization, the impact of cross-section library differences diminishes as the distance decreases. Therefore, $g(r)$ data by Rivard are used for $r < 1$ cm, and are italicized in Table II.

3.3. MED3631-A/M $F(r,\theta)$

Since $F(r,\theta)$ data are by definition normalized to a given distance and the impact of outdated photon cross-section libraries was assumed to be negligible, the Monte Carlo $F(r,\theta)$ results by Rivard are recommended as the consensus dataset since they covered the largest angular and radial ranges. While the dose distribution of this source model in the longitudinal plane is highly nonsymmetric in close proximity to the source, the $F(r,\theta)$ data were obtained using averaged dose-rate data above and below the transverse plane (supplementary angles) to account for the asymmetric geometric source model used by Rivard. These averaged results using the line source approximation with $L = 0.42$ cm are presented, and the MED3631-A/M $\phi_{\mathrm{an}}(r)$ results are presented in Table VII. Using the same active length, results by Rivard exhibited much less variation at $\theta \sim 90°$ than Wallace and Fan ($<1\%$ compared to 5%). This was expected since they used TLDs which were more susceptible to volume-averaging artifacts along the longitudinal axis. Agreement among converted $F(r,\theta$

Patel *et al.* The two values agree within the experimental uncertainties, and the $_{CON}\Lambda$ value is given in Table I.

4.2. I25.S06 $g(r)$

The $g(r)$ data calculated by Hedtjarn *et al.* and measured by Patel *et al.* are based upon a line source with $L = 0.35$ cm. These two datasets agree within experimental uncertainties (5%) except for $g(0.5)$. Due to its larger coverage of radial distance and closer coverage towards the source, the Monte Carlo $g(r)$ data of Hedtjarn *et al.* are recommended.

4.3. I25.S06 $F(r,\theta)$

Measured anisotropy functions by Patel *et al.*, based on an active length of 0.35 cm, were compared to Monte Carlo data by Hedtjarn *et al.* and Williamson.[42,44] For completeness, the anisotropy function derived from the 4 cm Monte Carlo calculations, which was omitted from the published paper, was added. Agreement within 5% was usually observed. The discrepancies were random and not indicative of different trends between the measured and computational approaches. The Hedtjarn *et al.* data are recommended and given in Table VIII.

5. Imagyn Medical Technologies Inc. *isostar* model IS-12501 ^{125}I source

International Isotopes Inc. (Denton, TX, now a division of Imagyn Medical Technologies Inc.), produced this source. It is marketed by Imagyn Medical Technologies, Inc. under the trade name ''*isostar* IS-12501.'' This source model first became available for analysis in 1999, and was introduced to clinical sites later that year. The design consists of five 0.56 mm diameter silver spheres on which ^{125}I silver iodide is adhered [Fig. 2(f)]. The silver spheres are encapsulated in a titanium tube whose ends are laser welded.

There are four pertinent references for this source.[38,39,128,129] Complete experimental and Monte Carlo results are given in Gearheart *et al.* and experimental results by Nath and Yue, respectively.[38,39] Experimental measurements (TLD in Solid Water™) of Λ, $g(r)$ from 0.5 cm to 10 cm, and anisotropy function at 2 cm and 5 cm were first reported by Gearheart *et al.* This work also contains Monte Carlo calculations of $g(r)$ and $F(r,\theta)$, both in water and in Solid Water™ with ratios between each media. These ratios were used to convert the TLD measurements of Λ in Solid Water™ to that in liquid water. The PTRAN Monte Carlo code was used, with the HUGO DLC-99 cross-section libraries. The bounded next-flight point-kerma estimator was used. Nath and Yue presented TLD measurements of Λ and $g(r)$ from 0.5 cm to 6 cm. Monte Carlo calculations were used to relate Λ in water to the measurements in Solid Water™.[37]

5.1. IS-12501 Λ

Ibbott and Nath explained that when the Λ value of Gearheart *et al.* is corrected using the revised 1999 NIST calibration, agreement with Nath and Yue improved to 3%. Ibbott and Nath published $_{CON}\Lambda = 0.940$ cGy h^{-1} U^{-1}, based upon the methodology in this protocol, and this value is given in Table I.

5.2. IS-12501 $g(r)$

Gearheart *et al.* and Nath and Yue measured $g(r)$ in Solid Water™. In both cases, $g(r)$ was calculated using the line-source approximation method. Gearheart *et al.* also published Monte Carlo calculation of $g(r)$ in liquid water. Analysis revealed the TLD measurements agreed with the Monte Carlo calculations within -8% to $+6\%$ with 1 standard deviation of $+4\%$ (1σ). Consequently, Gearheart *et al.* Monte Carlo values in water are recommended as $_{CON}g(r)$, and are listed in Table II.

5.3. IS-12501 $F(r,\theta)$

Nath and Yue did not measure $F(r,\theta)$. Gearheart *et al.* published TLD measurements in Solid Water™ and also performed Monte Carlo calculations in both Solid Water™ and liquid water. The geometry function was modeled as a line source with active length of 0.34 cm. Monte Carlo calculations were performed at 1, 2, 3, 5, and 7 cm to facilitate calculation of $\phi_{an}(r)$ at these distances. Comparison of measured and calculated data demonstrate good agreement within combined uncertainties of 10%. Consensus $F(r,\theta)$ and $\phi_{an}(r)$ data from Gearheart *et al.* are presented in Table IX.

6. Theragenics Corporation model 200 ^{103}Pd source

The model 200 (TheraSeed®) source was introduced by Theragenics Corporation in 1987, and remained the sole commercially available interstitial ^{103}Pd source until 1999. The encapsulation is a 0.056 mm thick Ti tube with a measured external length of 4.50 mm and average measured outer diameter of 0.83 mm, respectively [Fig. 2(g)]. The tube ends are closed by means of inverted ''end-cups'' composed of 0.040 mm thick Ti metal welded to the Ti tube. Using transmission radiography and microscopic examination,

including the original TG-43 protocol dataset for the model 200 source, are based upon the obsolete heavy seed geometry.[7,66,106,107]

Until 1999, there was no air-kerma strength standard for the model 200 source. Theragenics Corporation maintained an ‘‘apparent activity’’ standard based upon intercomparison of photon fluence rates from model 200

spacing. No information was given regarding the manner in which S_K was determined. However, the bounded next flight point kerma estimator was employed.

Rivard calculated the 2D dosimetry parameters using MCNP version 4B2 and the DLC-189 cross-section library similar to the MED3631-A/M calculations (accounting for motion of internal source components).[138] Results for $g(r)$ and $F(r,\theta)$ were evaluated over the 0.25 to 10 cm distance range, and $F(r,\theta)$ was evaluated from $0° \leqslant \theta \leqslant 180°$ in 1° increments (though only 10° increment data were reported). The Ti characteristic x-ray contributions were removed offline by binning kerma on energy and removing contributions <5 keV. The energy dependence of TG-43 dosimetry parameters was analyzed by discretizing the polyenergetic ^{103}Pd spectra, and performing comparisons with results presented by Chen and Nath, Luxton and Jozsef, and Carlsson and Ahnjesö.[109,139,140]

7.1. MED3633 Λ

Wallace and Fan reported a measured Λ value of 0.680 ± 0.033 cGy h^{-1} U^{-1}, yielding the value of 0.702 ± 0.034 cGy h^{-1} U^{-1} when corrected for the 1999 NIST WAFAC anomaly. Using a diode scanning system, a liquid water phantom, and an in-house cross-calibration technique, Li *et al.* reported two measured values (0.714 and 0.682 cGy h^{-1} U^{-1}) before applying the +3.2% 1999 NIST WAFAC anomaly correction (Table I). Though the corrected average of these two diode readings would yield 0.720 cGy h^{-1} U^{-1}, these measurements are not included in this consensus since a cross-calibration method using a source from a different manufacturer is discouraged. Therefore, Wallace and Fan gave $\Lambda = 0.702$ cGy h^{-1} U^{-1} with $_{EXP}\Lambda$ also equal to 0.702 cGy h^{-1} U^{-1}. Using MCPT, Li *et al.* calculated 0.677 cGy h^{-1} U^{-1}, and Rivard calculated 0.672 cGy h^{-1} U^{-1} using discretized photon energy fluence estimators. Consequently, $_{MC}\Lambda = 0.6745$ cGy h^{-1} U^{-1} was obtained. Combining results, $_{CON}\Lambda = 0.688$ cGy h^{-1} U^{-1} is shown in Table I.

7.2. MED3633 $g(r)$

While the MCNP results of Rivard covered the largest radial distance range and came closest to the source, the MCNP $g(r)$ results could not be recommended. As was the case for the MED3631-A/M source, Rivard used the default MCNP cross-section library which is now known to cause significant differences following radiation penetration through multiple pathlengths due to obsolete photon cross-section data. Thus, the $g(r)$ results of Li *et al.* generated using MCPT and updated cross-section data are recommended for $_{CON}g(r)$ data, with Rivard's data recommended (italicized) only for $r<1$ cm (Table III) where cross-section data selection was less crucial. Note that the Rivard $g(0.5)$ data exactly matched that of Li *et al.*, i.e., $g(0.5)=1.243$. For $r>4$ cm the Rivard data differed from the Li *et al.* data by more than 10%, while Wallace and Fan $g(r)$ data agreed with the Li *et al.* data (except at $r=6$ cm where the diode signal was quite low) within $\pm 4\%$. Compared to the Li *et al.* MCPT data, the Li *et al.* diode data varied by $\pm 7\%$ for $0.5<r<1.5$ cm, and are not considered reliable. Therefore the $_{CON}g(r)$ is a combination of results by Rivard at close distances and Li *et al.* for $r>1$ cm.

7.3. MED3633 $F(r,\theta)$

Rivard's MED3633 $F(r,\theta)$ dataset covered the largest angular and radial ranges, and its accuracy was expected not to be influenced by the outdated photon cross-section libraries since data were normalized to a given distance. As for the MED3631-A/M source, the dose rate data above and below the transverse plane were averaged to account for the asymmetric geometric source model, and used to derive the consensus dataset 2D anisotropy function data (Table XI). These averaged data were compared with the Monte Carlo data by Li *et al.* and the TLD results from Wallace and Fan at common radial distances of 1, 2, and 5 cm. Over these radii, the Li *et al.* results agreed with Rivard's data within $\pm 7\%$ (typically $+4\%$). While differences as large as 20% were noted for small polar angles, these discrepancies may be attributed to different source models or the averaging technique used for the $F(r,\theta=0°-180°)$ data. In comparison to the MCNP results, the $F(r,\theta)$ dataset of Wallace and Fan exhibited unexpected irregularities ($+13\%$ at $r=5$ cm, $\theta=80°$, and $+18\%$ at $r=1$ cm, $\theta=40°$).

APPENDIX B: NIST AIR-KERMA STRENGTH STANDARDS FOR LOW-ENERGY PHOTON-EMITTING SOURCES

1. NIST 1985 standard using the free-air chamber

The National Institute of Standards and Technology (NIST) maintains the U.S. primary air-kerma standards for x rays in the energy range of 10 to 300 keV and for photon-emitting radionuclides such as ^{137}Cs, ^{192}Ir, ^{103}Pd, and ^{125}I. The primary standard for ^{137}Cs and ^{192}Ir sources consists of Bragg–Gray cavity chambers.[141] To provide similar traceability for low-energy photon-emitting ^{125}I sources, Loftus developed a primary standard for ^{125}I sources in 1985 based on the Ritz parallel-plate free-air chamber (FAC), the national primary x-ray standard for superficial therapy beams.[142,143] This chamber was used to measure the exposure rate in free-space on the transverse plane of model 6711 and 6702 sources. Because the Ritz FAC background current was high relative to signal strength expected from a single source, this device was limited to a calibration arrangement of a combination of 4 to 6 sources. These calibrations were then transferred to a spherical aluminum re-entrant ionization chamber which served as the secondary standard for routine calibrations.[144] Uncertainties ($2\sigma=95\%$ confidence level) for the transferred measurements were 3% and 4% for the model 6702 and 6711 ^{125}I sources, respectively. Measurement uncertainties for subsequent source calibrations using the re-entrant chamber were estimated to be 5% and 6% for the 6702 and 6711 sources, respectively.[144] This Loftus calibration standard became available in 1985 and has been referred to as the NIST 1985 air-kerma strength standard

($S_{K,N85}$) in recent AAPM guidance protocols.[36,145] Soon after introduction of this standard, Kubo called attention to the influence on exposure measurements made in air by Ti *K*-shell characteristic x rays.[146] These low-energy x rays (<5 keV) are clinically insignificant because they are largely absorbed by tissue or water within 1 mm of the source. However, these x rays can affect air-kerma strength measurements. Because of the extreme difficulty in using the Ritz FAC for such measurements, NIST chose not to repeat this standardization process until a new instrument could brements,

evidence is persuasive. In the case of the model 200 source,[36,145] normalizing to point air-kerma strength calculations leads to dose-rate constant values that are sensitive to small changes in internal source geometry and differ from experimental measurements by as much as 17%. Similar but smaller effects of $\sim 5\%$ occur for the models 6711 and STM1251 ^{125}I sources.[25,149] In contrast, Monte Carlo simulations incorporating the WAFAC measurement geometry reveal no such sensitivity, and result in dose-rate constant (Sec. III A 2) values having close agreement with experimental measurements.[131] Furthermore, significant anisotropy implies that any air-kerma rate measurements based upon a point detector will have large uncertainties due to sensitivity to source alignment and deviation of the actual source geometry from its idealized specifications. Despite its metrological impurity, the current WAFAC standard serves the clinical community well and has many advantages over previous standards. By averaging air-kerma strength over regions of significant and possibly poorly reproducible anisotropy near the source transverse-plane, dosimetric uncertainties caused by misalignment and source geometry specification uncertainties are substantially mitigated.

During the development and testing of the WAFAC in 1997–1998, extensive intercomparisons were made between the WAFAC and the NIST re-entrant chamber (the Loftus transfer standard) for Models 6702 and 6711 sources. The results from 10 sources established a ratio of the new NIST WAFAC standard ($S_{K,N99}$) to the old Loftus standard ($S_{K,N85}$) of 0.898 ± 0.014 for 6702 sources and 0.896 ± 0.010 for 6711 sources, and 0.897 ± 0.011, combining the two models. Based on this average, the AAPM recommended using $(S_{K,N99})/(S_{K,N85}) = 0.897$ to convert between the two standards for all applicable ^{125}I source models (Amersham 6711 and 6702 and NASI models 3631 A/S and A/M).[36] Because they were so tedious, NIST discontinued periodic intercomparisons of Loftus re-entrant chamber and WAFAC measurements in 1999. In preparation for the introduction of the new $S_{K,N99}$ standard, [illegible] (1999) 511–528.

standard) and in the re-entrant chamber (NIST 1985 standard). The results indicate a combined ratio for the sources of 0.897 ± 0.028, in very good agreement with the determination made in 1997–1998. This then confirmed the correctness of the WAFAC measurements in 2000–2001 and in 1997–1998, and indicated that the problem was confined to measurements made in 1999 (perhaps including late 1998).

The conclusion is that NIST WAFAC measurements up to mid-1998 and after January 1 2000 are correct, and that current dose-rate constants for the 6702 and 6711 sources, based on the ratio NIST1999/NIST1985 $= 0.897$, are valid. However, WAFAC air-kerma strengths measured in 1999 were too large by 2% to 7%, and required dose-rate constant measurements normalized to NIST 1999 S_K calib(0.89snofm46.be-453.1(st319)]TJ -15.020revis7.4(c2 T0.8c(ar-332ly)-648 0.453. 0 TD (S)T

$$\dot{D}(r)=S_K\cdot\Lambda\cdot\left(\frac{r_0}{r}\right)^2\left(\frac{g_L(r)}{g_L(r_{\min})}\right)\cdot g_P(r_{\min})\cdot\phi_{\text{an}}(r_{\min}),$$

$$r<r_{\min}. \tag{C4}$$

No matter how sophisticated an extrapolation model is chosen, users should realize that at $r<0.25$ cm where $\phi_{\text{an}}(r)$ data may not be available due to lack of assessment or due to positioning within the capsule, none of the 1D models described above yield quantitatively meaningful estimates of the solid angle-weighted average dose.

APPENDIX D: ANISOTROPY CONSTANT

The definition of the anisotropy constant, $\overline{\phi}_{\text{an}}$, largely remains the same as that presented in TG-43, and is expanded upon. Use of $\overline{\phi}_{\text{an}}$, as commonly practiced at this time, does not exactly reproduce either the measured or Monte Carlo dosimetry data for $r<1$ cm. Therefore, it is strongly recommended that users utilize $\phi_{\text{an}}(r)$ and Eq. (11), or compensate for treatment planning inadequacies using the method outlined in Eq. (14), for implementing 1D dosimetry formalism.

For those users who insist on using $\overline{\phi}_{\text{an}}$, the following implementation will minimize dose-calculation errors at small distances, e.g., $r\leqslant 1$ cm:

$$\dot{D}(r)=S_K\cdot\Lambda\cdot\left(\frac{r_0}{r}\right)^2\cdot g_L(r)\cdot\overline{\phi}_{\text{an}}. \tag{D1}$$

For this purpose, the inverse-square law weighted average of $\phi_{\text{an}}(r)$ for $r>1$ cm should be used,

$$\overline{\phi}_{\text{an}}=\frac{\sum_{r\geqslant 1\text{ cm}}^{r_{\max}}\phi_{\text{an}}(r)\cdot r^{-2}}{\sum_{r\geqslant 1\text{ cm}}^{r_{\max}}r^{-2}}. \tag{D2}$$

For instances where $\phi_{\text{an}}(r)$ data are not available over constant increments of r, linear interpolation of $\phi_{\text{an}}(r)$ may be used for derivation of $\overline{\phi}_{\text{an}}$. The constraint on r is needed because dose distributions near typical brachytherapy sources generally take the shape of prolate ellipsoids due to the dominating effects of solid angle. This is because $F(r,\theta)$ excludes dose fall-off already included by the geometry function, and $\phi_{\text{an}}(r)$ (and subsequently $\overline{\phi}_{\text{an}}$) do not. Therefore, $\phi_{\text{an}}(r)$ rapidly increases as $r<2L$, and can assume values much larger than unity. While nonintuitive, the use of $g_L(r)$ with the point-source geometry function in Eq. (D1) better approximates the average dose at small distances than the superficially more consistent expression $g_X(r)\cdot G_X(r,\theta_0)\cdot\overline{\phi}_{\text{an}}\cdot G_X(r_0,\theta_0)^{-1}$ again due to the ellipsoidal shape of the isodose surfaces. Thus $r^{-2}\cdot\overline{\phi}_{\text{an}}\approx G(r,\theta_0)\cdot\phi_{\text{an}}(r)$. For sources with $L\approx 0.3$ cm, this approximation is sufficiently good that errors introduced are often less than 5% at distances <0.3 cm.[150–152] However, Williamson demonstrated that Eq. (D1) can produce much larger errors for low-energy sources with longer effective active lengths.[44] Because of this short-distance behavior, the following forms should not be used at $r<0.5$ cm:

$$\dot{D}(r)=S_K\cdot\Lambda\cdot\left(\frac{r_0}{r}\right)^2\cdot g_P(r)\cdot\overline{\phi}_{\text{an}}.$$

or

$$D(r)=S_K\cdot\Lambda\cdot\frac{G_L(r,\theta_0)}{G_L(r_0,\theta_0)}\cdot g_L(r)\cdot\overline{\phi}_{\text{an}}. \tag{D3}$$

APPENDIX E: APPARENT ACTIVITY

The quantity apparent activity, A_{app}, is defined as the activity of an unfiltered point source of a given radionuclide that has the same air-kerma strength as that of the given encapsulated source. It has been widely used by vendors and customers alike to specify the strength of sealed radioactive sources such as ^{125}I, ^{103}Pd and ^{198}Au. Furthermore, A_{app} is used in the treatment planning of permanent implants using ^{103}Pd and ^{125}I interstitial sources. Using the apparent activity as a method of source strength specification suffers from a number of problems. For example, vendors using apparent activity to report source strength in essence convert a statement of source output, e.g., S_K, into A_{app} by dividing S_K by an assumed value of the exposure rate constant $(\Gamma_\delta)_X$. To calculate absorbed dose in a medium around such sources, users shall multiply the vendor supplied A_{app} value by the same $(\Gamma_\delta)_X$ value. Although $(\Gamma_\delta)_X$ is a clearly defined physical concept, it has no meaningful physical role in the dosimetry of output calibrated sources. Continued use of such dummy constants constitutes a significant potential source of dosimetric error since the user may choose the wrong $(\Gamma_\delta)_X$ value. It is essential that users employ the same $(\Gamma_\delta)_X$ values as the manufacturer for dosimetric calculations rather than more physically accurate or definitive values taken from the recent literature.

In 1999, NIST implemented a new primary standard for air-kerma strength.[8] The AAPM has consistently taken the position that S_K should be the quantity used for specifying brachytherapy source strength for the purpose of defining calibration standards, documenting source strength on calibration reports and for all aspects of dose calculation and treatment prescription. Both users and vendors shall take appropriate steps to adopt this new source-strength standard correctly. To facilitate an unambiguous conversion of source strength estimates and for transitional practice, the LIBD has recommended a set of data and equations for the conversion of (S_K/A_{app}) for ^{125}I and ^{103}Pd interstitial brachytherapy sources. For all ^{125}I and ^{103}Pd sources, regardless of internal construction, the values of $(\Gamma_\delta)_X$ recommended were 1.45 and 1.476 R cm^2 mCi^{-1} h^{-1}, respectively. When implementing the TG-43 formalism based upon apparent activity specification, the recommended (S_K/A_{app}) conversion coefficients were 1.270 and 1.293 μGy m^2 h^{-1} mCi^{-1} for ^{125}I and ^{103}Pd, respectively. The authors discussed the importance of using a consistent set of values for the exposure rate constant $(\Gamma_\delta)_X$ for the evaluation of (S_K/A_{app}).[8] For example, adopting S_K-to-A_{app} conversion coefficients derived from modern $(\Gamma_\delta)_X$ values, different from the ones used by the authors; would require all users and vendors to redefine the relationship between S_K and A_{app}; would require updating of dosi-

metric constants in all A_{app}-based treatment planning systems; could cause significant confusion among clinical users; would complicate future retrospective analyses of clinical outcome data; and would not improve dosimetric accuracy. This further emphasizes the importance of using the same value of $(\Gamma_\delta)_X$ by the vendors and the users. Consequently, the AAPM continues to recommend that the quantity A_{app} not be used for specification of brachytherapy source strength.

[1] R. Nath, L. L. Anderson, G. Luxton, K. A. Weaver, J. F. Williamson, and A. S. Meigooni, ''Dosimetry of interstitial brachytherapy sources: Recommendations of the AAPM Radiation Therapy Committee Task Group No. 43,'' Med. Phys. **22**, 209–234 (1995).

[2] Interstitial Collaborative Working Group (ICWG), in *Interstitial Brachytherapy: Physical, Biological, and Clinical Considerations*, edited by L. L. Anderson, R. Nath, K. A. Weaver, D. Nori, T. L. Phillips, Y. H. Son, S-T. Chiu-Tsao, A. S. Meigooni, J. A. Meli, and V. Smith (Raven Press, New York, 1990).

[3] J. F. Williamson, ''Physics of brachytherapy,'' in *Principles and Practice of Radiation Oncology*, edited by C. A. Perez and L. W. Brady, 3rd ed. (Lippincott-Raven Press, Philadelphia, 1997) pp. 405–467.

[4] A. S. Meigooni and R. Nath, ''Response to 'Comment on Dosimetry of interstitial brachytherapy sources: Recommendations of the AAPM Radiation Therapy Committee Task Group No. 43','' Med. Phys. **27**, 265 (2000).

[5] R. W. Kline, ''Comment on 'Dosimetry of interstitial brachytherapy sources: Recommendations of the AAPM Radiation Therapy Committee Task Group No. 43','' Med. Phys. **23**, 1579 (1996).

[6] A. Y. C. Fung, ''Comment on 'Dosimetry of interstitial brachytherapy sources: Recommendations of the AAPM Radiation Therapy Committee Task Group No. 43','' Med. Phys. **25**, 2477 (1998).

[7] J. F. Williamson, B. M. Coursey, L. A. DeWerd, W. F. Hanson, R. Nath, M. J. Rivard, and G. Ibbott, ''Recommendations of the American Association of Physicists in Medicine on ^{103}Pd interstitial source calibration and dosimetry: Implications for dose specification and prescription (AAPM Report No. 69),'' Med. Phys. **27**, 634–642 (2000).

[8] J. F. Williamson, B. M. Coursey, L. A. DeWerd, W. F. Hanson, R. Nath, M. J. Rivard, and G. Ibbott, ''On the use of apparent activity (A_{app}) for treatment planning of ^{125}I and ^{103}Pd interstitial brachytherapy sources: Recommendations of the American Association of Physicists in Medicine Radiation Therapy Subcommittee on Low-Energy Brachytherapy Source Dosimetry,'' Med. Phys. **26**, 2529–2530 (1999).

[9] J. F. Williamson, B. M. Coursey, L. A. DeWerd, W. F. Hanson, and R. Nath, ''Dosimetric prerequisites for routine clinical use of new low energy photon interstitial brachytherapy sources,'' Med. Phys. **25**, 2269–2270 (1998).

[10] Radiological Physics Center, The M.D. Anderson Cancer Center, Houston, TX http://rpc.mdanderson.org/rpc/htm/Home_htm/Low-energy.htm last accessed December 1, 2003.

[11] B. S. Hilaris, D. Nori, and L. L. Anderson, *Atlas of Brachytherapy* (MacMillan Publishing Co., New York, 1988).

[12] W. Lee, B. D. T. Daly, T. A. DiPetrillo, D. M. Morelli, A. C. Neuschatz, J. Morr, and M. J. Rivard, ''Limited resection for non-small cell lung cancer: Observed local control with implantation of I-125 brachytherapy seeds,'' Ann. Thorac. Surg. **75**, 237–243 (2003).

[13] Y. Yu, L. L. Anderson, Z. Li, D. E. Mellenberg, PR Math, Me MSchlle D. MeJeaeri'LPr

[37] J. F. Williamson, "Comparison of measured and calculated dose rates in water near I-125 and Ir-192 seeds," Med. Phys. **18**, 776–786 (1991).
[38] D. M. Gearheart, A. Drogin, K. Sowards, A. S. Meigooni, and G. S. Ibbott, "Dosimetric characteristics of a new ^{125}I brachytherapy source," Med. Phys. **27**, 2278–2285 (2000).
[39] R. Nath and N. Yue, "Dose distribution along the transverse axis of a new ^{125}I source for interstitial brachytherapy," Med. Phys. **27**, 2536–2540 (2000).
[40] J. I. Monroe and J. F. Williamson, "Monte Carlo-aided dosimetry of the Theragenics TheraSeed® Model 200 ^{103}Pd interstitial brachytherapy seed," Med. Phys. **29**, 609–621 (2002).
[41] B. N. Taylor and C. E. Kuyatt, "Guidelines for evaluating and expressing the uncertainty of NIST measurement results," NIST Technical Note 1297 (U.S. Government Printing Office, Washington, DC, 1994).
[42] H. Hedtjarn, G. A. Carlsson, and J. F. Williamson, "Monte Carlo-aided dosimetry of the Symmetra model 125.S06 ^{125}I, interstitial brachytherapy seed," Med. Phys. **27**, 1076–1085 (2000).
[43] J. H. Hubbell, "Review of photon interaction cross section data in the medical and biological context," Phys. Med. Biol. **44**, R1–R2 (1999).
[44] J. F. Williamson, "Dosimetric characteristics of the DraxImage Model LS-1 I-125 interstitial brachytherapy source design: A Monte Carlo investigation," Med. Phys. **29**, 509–521 (2002).
[45] M. J. Rivard, "Monte Carlo calculations of AAPM Task Group Report No. 43 dosimetry parameters for the MED3631-A/M ^{125}I source," Med. Phys. **28**, 629–637 (2001).
[46] J. F. Williamson, "Monte Carlo modeling of the transverse-axis dose distribution of the Model 200 ^{103}Pd interstitial brachytherapy source," Med. Phys. **27**, 643–654 (2000).
[47] M. S. Levenson, D. L. Banks, K. R. Eberhardt, L. M. Gill, W. F. Guthrie, H. K. Liu, M. G. Vangel, J. H. Yen, and N. F. Zhang, "An approach to combining results from multiple methods motivated by the ISO GUM," J. Res. Natl. Inst. Stand. Technol. **105**, 571–579 (2000).
[48] Z. Li, J. J. Fan, and J. R. Palta, "Experimental measurements of dosimetric parameters on the transverse axis of a new ^{125}I source," Med. Phys. **27**, 1275–1280 (2000).
[49] Z. Li, J. F. Williamson, and H. Perera, "Monte Carlo calculation of kerma-to-a-point in the vicinity of media interfaces," Phys. Med. Biol. **38**, 1825–1840 (1993).
[50] T. Kron, L. DeWerd, P. Mobit, J. Muniz, A. Pradhan, M. Toivonen, and M. Waligorski, "A checklist for reporting of thermoluminescence dosimetry (TLD) measurements," Phys. Med. Biol. **44**, L15–L17 (1999).
[51] J. F. Williamson, "Monte Carlo evaluation of specific dose constants in water for ^{125}I seeds," Med. Phys. **15**, 686–694 (1988).
[52] National Nuclear Data Center. Nuclear data from NuDat, a web-based database maintained by the National Nuclear Data Center, Brookhaven National Laboratory, Upton, NY, USA; last database update reported as August 12, 2000; http://www.nndc.bnl.gov/nndc/nudat/ last accessed February 17, 2004.
[53] Lund/LBNL Nuclear Data Search (1999). Version 2.0, February 1999, by S. Y. F. Chu, L. P. Ekström, and R. B. Firestone, providing the WWW Table of Radioactive Isotopes, maintained by the Lawrence Berkeley National Laboratory, Berkeley, CA, USA, and the Department of Physics, Lund University, Sweden; http://nucleardata.nuclear.lu.se/nucleardata/toi/ last accessed February 17, 2004.
[54] S. M. Seltzer, "Calculation of photon mass energy-transfer and mass energy-absorption coefficients," Radiat. Res. **136**, 147–170 (1993).
[55] S. M. Seltzer and J. H. Hubbell, "Tables and graphs of mass attenuation coefficients and mass energy-absorption coefficients for photon energies 1 keV to 20 MeV for elements $Z=1$ to 92 and some dosimetric materials," Japanese Society of Radiological Technology, ISSN 1340-7716 (1995).
[56] M. J. Rivard, D. S. Waid, and J. G. Wierzbicki, "Mass attenuation coefficients of Clear-Pb® for photons from ^{125}I, ^{103}Pd, ^{99m}Tc, ^{192}Ir, ^{137}Cs, and ^{60}Co," Health Phys. **77**, 571–578 (1999).
[57] ICRU 37 Stopping Powers for Electrons and Positrons, International Commission on Radiation Units and Measurements (ICRU 37, Bethesda, MD, 1989).
[58] Private communication with Steve Seltzer of NIST, September 13, 2001.
[59] N. S. Patel, S-T. Chiu-Tsao, J. F. Williamson, P. Fan, T. Duckworth, D. Shasha, and L. B. Harrison, "Thermoluminescent dosimetry of the Symmetra™ ^{125}I model I25.S06 interstitial brachytherapy seed," Med. Phys. **28**, 1761–1769 (2001).
[60] S.-T. Chiu-Tsao and L. L. Anderson, "Thermoluminescent dosimetry for ^{103}Pd seeds (model 200) in solid water phantom," Med. Phys. **18**, 449–452 (1991).
[61] A. S. Meigooni, V. Mishra, H. Panth, and J. F. Williamson, "Instrumentation and dosimeter-size artifacts in quantitative thermoluminescent dosimetry of low-dose fields," Med. Phys. **22**, 555–561 (1995).
[62] L. da Rosa and H. Nette, "Thermoluminescent dosimeters for exposure assessment in gamma or x radiation fields with unknown spectral distribution," Appl. Radiat. Isot. **39**, 191–197 (1988).
[63] R. K. Das, Z. Li, H. Perera, and J. F. Williamson, "Accuracy of Monte Carlo photon transport simulation in characterizing brachytherapy dosimeter energy response artifacts," Phys. Med. Biol. **41**, 995–1006 (1996).
[64] J. F. Williamson, J. F. Dempsey, A. S. Kirov, J. I. Monroe, W. R. Binns, and H. Hedtjärn, "Plastic scintillator response to low-energy photons," Phys. Med. Biol. **44**, 857–872 (1999).
[65] M. Schell, C. C. Ling, Z. C. Gromadzki, and K. R. Working, "Dose distributions of model 6702 I-125 seeds in water," Int. J. Radiat. Oncol., Biol., Phys. **13**, 795–799 (1987).
[66] S-T. Chiu-Tsao, L. L. Anderson, K. O'Brien, and R. Sanna, "Dose rate determination for ^{125}I seeds," Med. Phys. **17**, 815–825 (1990).
[67] A. Piermattei, L. Azario, G. Monaco, A. Soriani, and G. Arcovito, "*p*-type silicon detector for brachytherapy dosimetry," Med. Phys. **22**, 835–839 (1995).
[68] J. F. Williamson, H. Perera, Z. Li, and W. R. Lutz, "Comparison of calculated and measured heterogeneity correction factors for ^{125}I, ^{137}Cs, and ^{192}Ir brachytherapy sources near localized heterogeneities," Med. Phys. **20**, 209–222 (1993).
[69] M. Ahmad, D. P. Fontenla, S-T. Chiu-Tsao, C. S. Chui, J. E. Reiff, L. L. Anderson, D. Y. C. Huang, and M. C. Schell, "Diode dosimetry of models 6711 and 6712 ^{125}I seeds in a water phantom," Med. Phys. **19**, 391–399 (1992).
[70] C. C. Ling, M. C. Schell, and E. D. Yorke, "Two-dimensional dose distribution of ^{125}I seeds," Med. Phys. **12**, 652–655 (1985).
[71] T. D. Bohm, D. W. Pearson, and R. K. Das, "Measurements and Monte Carlo calculations to determine the absolute detector response of radiochromic film for brachytherapy dosimetry," Med. Phys. **28**, 142–146 (2001).
[72] A. Niroomand-Rad, C. R. Blackwell, B. M. Coursey, K. P. Gall, J. M. Galvin, W. L. McLaughlin, A. S. Meigooni, R. Nath, J. E. Rogers, and C. G. Soares, "Radiochromic film dosimetry: Recommendations of AAPM Radiation Therapy Committee Task Group 55," Med. Phys. **25**, 2093–2115 (1998).
[73] D. Flühs, M. Heintz, F. Indenkämpen, C. Wieczorek, H. Kolanoski, and U. Quast, "Direct reading measurement of absorbed dose with plastic scintillators—The general concept and applications to ophthalmic plaque dosimetry," Med. Phys. **23**, 427–434 (1996).
[74] A. S. Kirov, C. Hurlbut, J. F. Dempsey, S. B. Shrinivas, J. W. Epstein, W. R. Binns, P. F. Dowkontt, and J. F. Williamson, "Towards two-dimensional brachytherapy dosimetry using plastic scintillator: New highly efficient water equivalent plastic scintillator materials," Med. Phys. **26**, 1515–1523 (1999).
[75] S-T. Chiu-Tsao, A. de la Zerda, J. Lin, and J. H. Kim, "High-sensitivity GafChromic film dosimetry for ^{125}I seed," Med. Phys. **21**, 651–657 (1994).
[76] J. F. Dempsey, D. A. Low, A. S. Kirov, and J. F. Williamson, "Quantitative optical densitometry with scanning-laser film digitizers," Med. Phys. **26**, 1721–1731 (1999).
[77] G. H. Chan and W. V. Prestwich, "Dosimetric properties of the new ^{125}I BrachySeed™ model LS-1 source," Med. Phys. **29**, 190–200 (2002).
[78] M. J. Maryanski, G. S. Ibbott, P. Eastman, R. J. Schulz, and J. C. Gore, "Radiation therapy dosimetry using magnetic resonance imaging of polymer gels," Med. Phys. **23**, 699–705 (1996).
[79] M. F. Chan, A. Y. C. Fung, Y-C. Hu, C-S. Chui, H. Amols, M. Zaider, and D. Abramson, "The measurement of three dimensional dose distribution of a ruthenium-106 ophthalmological applicator using magnetic resonance imaging of BANG polymer gels," J. Appl. Clin. Med. Phys. **2**, 85–89 (2001).
[80] B. F. Hasson, "Chemical dosimetry in the near-zone of brachytherapy sources," Med. Phys. **25**, 2076 (1998).
[81] A. S. Meigooni, Z. Bharucha, M. Yoe-Sein, and K. Sowards, "Dosimetric characteristics of the Best® double-wall ^{103}Pd brachytherapy source," Med. Phys. **28**, 2568–2575 (2001).

[82] A. S. Meigooni, Z. Li, Vi. Mishra, and J. F. Williamson, ''A comparative study of dosimetric properties of Plastic Water and Solid Water in brachytherapy applications,'' Med. Phys. **21**, 1983–1987 (1994).
[83] J. F. Williamson and A. S. Meigooni, ''Quantitative dosimetry methods in brachytherapy,'' in *Brachytherapy Physics*, edited by J. F. Williamson, B. R. Thomadsen, and R. Nath (Medical Physics Publishing, Madison, WI, 1995), pp. 87–133.
[84] A. S. Meigooni, J. A. Meli, and R. Nath, ''A comparison of solid phantoms with water for dosimetry of ^{125}I model 6702 brachytherapy sources,'' Med. Phys. **15**, 695–701 (1988).
[85] K. A. Weaver, ''Response of LiF powder to ^{125}I photons,'' Med. Phys. **11**, 850–854 (1984).
[86] C. Reft, ''The energy response of LiF TLD-100 to low and high energy photons and to high energy electrons for varying dosimeter thickness,'' Phys. Med. Biol. **33**, 96 (1988).
[87] A. S. Meigooni, D. M. Gearheart, and K. Sowards, ''Experimental determination of dosimetric characteristics of Best double-walled I-125 brachytherapy source'' Data sheet provided by Best Industries, October 2,

mination of dose rate constant,'' Med. Phys. **29**, 1637–1638 (2002).
[130] J. F. Williamson, B. M. Coursey, L. A. DeWerd, W. F. Hanson, G. Ibbott, R. Nath, and M. J. Rivard, ''Important notice for radiation therapy physicists using ^{125}I or ^{103}Pd brachytherapy sources,'' Radiation Therapy Committee on Low-Energy Interstitial Brachytherapy Dosimetry Subcommittee, Recommendations of the American Association of Physicists in Medicine, http://rpc.mdanderson.org/rpc/htm/Home_htm/Low-energy%20documents/ImpNotice_EndUsers_v12.pdf last accessed February 17, 2004.
[131] R. Nath, N. Yue, K. Shahnazi, and P. J. Bongiorni, ''Measurement of dose-rate constant for ^{103}Pd seeds with air kerma strength calibration based upon a primary national standard,'' Med. Phys. **27**, 655–658 (2000).
[132] A. S. Meigooni, S. Sabnis, and R. Nath, ''Dosimetry of ^{103}Pd brachytherapy sources for permanent implant,'' Endocurietherapy/Hyperthermia Oncology **6**, 107–117 (1990).
[133] N. Yue and R. Nath, ''Experimental determination of the anisotropy function for the Model 200 ^{103}Pd ''light seed'' and derivation of the anisotropy constant based upon the linear quadratic model,'' Med. Phys. **29**, 1120–1129 (2002).
[134] R. E. Wallace and J. J. Fan, ''Dosimetric characterization of a new design ^{103}palladium brachytherapy source,'' Med. Phys. **26**, 2465–2470 (1999).
[135] G. Luxton, ''Comparison of radiation dosimetry in water and solid phan-